PRESSURE DROP IN ADIABATIC, TWO-PHASE, TWO-COMPONENT FLOW IN 180 DEGREE BENDS

BY

NITAI KRUSHNA GIRI

DEPARTMENT OF MECHANICAL ENGINEERING

INDIAN INSTITUTE OF TECHNOLOGY KANPUR

AUGUST, 1972

PRESSURE DROP IN ADIABATIC, TWO-PHASE, TWO-COMPONENT FLOW IN 180 DEGREE BENDS

A Thesis Submitted
In Partial Fulfilment of The
Requirements For the
Degree of

MASTER OF TECHNOLOGY

by
NITAI KRUSHNA GIRI

to the
Department of Mechanical Engineering
Indian Institute of Technology, Kanpur

August, 1972

CERTIFICATE

This is to certify that this work on "Pressure Drop in Adiabatic, Two-phase, Two-component Flow in 180 Degree Bends" has been carried out under my supervision and has not been submitted elsewhere for a degree.

V. Kadambi

V. KADAMBI
Associate Professor
Department of Mechanical Engineering
Indian Institute of Technology, Kanpur

ACKNOWLEDGEMENT

The author wishes to place on record his deep sense of gratitude and indebtedness to Dr.V.Kadambi, for his keen interest, and stimulating prompt discussions throughout this investigation.

The author is also grateful to Mr.M.Prasad for his help, encouragement and discussions during this work.

The author conveys his sincere thanks to his friend, Sri Ravichandran for his assistance in making observations and calculations, and to Sri P.N. Mishra of Refrigeration and Airconditioning Laboratory for his help in fabrication, and setting up the experimental apparatus.

The author also takes this opportunity to convey his thanks to the following : to the staff of the Central Glass Blowing Shop, Central Workshop and Fabrication Shop and Messrs, M.M. Singh, B.S. Arya, C.P. Singh and S.Chakrapani of Mechanical Engineering Department Laboratories, for their cooperation and help during the course of this undertaking. He is also thankful to Sri Uma Raman Pandey for his efficient typing of the manuscript. Lastly the author expresses his appreciation and thanks to Mr. S.C. Angrish of Chemical Engineering for taking splendid photographs.

ABSTRACT

This work deals with the experimental investigation of two-phase flow of air-water mixture at room temperature and pressures close to atmospheric in a series of 180 degree bends in a horizontal plane. The bends are made of glass tubes of 11.6 and 16.2 mm internal diameter, with curvature-to-tube diameter ratios (D/d) varying from 6.18 to 22.4. Various two-phase flow patterns have been observed and pressure drops determined as a function of air and water flow rates and curvature-to-tube diameter ratios, with annular flow in all the bends.

The flow patterns observed for two-phase flow in 180° bends are similar to those for horizontal pipes in two-phase flow. It is observed that the transition from one flow pattern to another is affected by diameter of the tube, curvature of the bend, water flow rate and air flow rate. The pressure drop for annular flow has been correlated using Lockhart-Martinelli parameters and D/d ratios. It is found that for the flow conditions and the geometry considered in the present work, the Lockhart-Martinelli plot can predict pressure drop within ± 20% accuracy. Compared with the Lockhart-Martinelli plot, the present results exhibit a slight dependence on liquid flow rates.

CONTENTS

NOMENCLATURE

A	Cross sectional area, m^2
A_l	Area occupied by liquid, m^2
A_g	Area occupied by gas, m^2
b	Width of duct, m
c	Constant
D	Diameter of curvature of bend, mm
d	Diameter of the pipe or test section, mm
d_e	Equivalent diameter of the flow channel, m
f	Friction factor for pipe, $\left[\Delta p/(\rho v^2/2)\right](d/l)$
f_s	Friction factor for straight pipe
f_c	Friction factor for curved pipe
$\bar{f}_{fr}$	Frication factor for two-phase flow in a straight duct
$\bar{f}_{loc}$	Local resistance coefficient for two-phase flow in an elbow
f_{loc}	Local resistance coefficient for single-phase flow in an elbow
f_{LO}	Friction factor due to the liquid flow with total mass velocity
G	Mass velocity equal to the total mass flow rate per unit pipe cross-sectional area, $kg/h\text{-}m^2$

G_l	Mass velocity of the liquid phase based on pipe cross sectional area, kg/h-m^2
G_g	Mass velocity of the vapor phase based on pipe cross sectional area, kg/h-m^2
g	Gravitational acceleration, m/h^2
g_c	Constant, kg-m/kg_f-h^2
h_w	Manometer reading in cm. of water
k	Constant
L	Length coordinate in the direction of flow, m
l	Axial length, m
$\dot{m}_t$	Total flow rate, kg/h
$\dot{m}_l$	Liquid flow rate, kg/h
$\dot{m}_g$	Gas flow rate, kg/h
$\dot{m}_{sus}$	Amount of moisture suspended in the flow, kg/h
P	Static pressure, kg_f/m^2
$\triangle P$ or dP	Pressure Drop, kg_f/m^2
$\triangle P_{TP}$	Total two-phase pressure drop, kg_f/m^2
$\triangle P_{TPF}$	Two-phase friction pressure drop, kg_f/m^2
$\triangle P_{LPF}$	Single-phase friction pressure drop due to flow of liquid with liquid mass velocity, kg_f/m^2
$\triangle P_{GPF}$	Single-phase friction pressure drop due to flow of gas with gas mass velocity, kg_f/m^2

ΔP_{LO}	Single-phase friction pressure drop due to flow of liquid with total mass velocity, kg_f/m^2
ΔP_{TPA}	Two-phase acceleration pressure drop, kg_f/m^2
ΔP_{TPG}	Two-phase gravitation pressure drop, kg_f/m^2
ΔP_{fr}	Two-phase pressure drop in a straight duct kg_f/m^2
ΔP_{turn}	Two-phase pressure drop due to deformation in velocity field as in turns, kg_f/m^2
$\frac{\Delta P}{\Delta L}$	Two-phase pressure gradient, kg_f/m^2-m
R	Radius of curvature of the bends, mm
Re	Reynolds number
Re_g	Reynolds number for gas phase flow alone in pipe = $G_g\ d_e/\mu_g$
Re_l	Reynolds number for liquid phase flow alone in pipe = $G_l d_e/\mu_l$
T	Temperature, K
v_l	Mean liquid velocity, m/h
v_g	Mean gas velocity, m/h
X	Correlation function of Lockhart-Martinelli
X_{tt}	Correlation function for turbulent gas to turbulent liquid flow
x	Quality of gas, $\dot{m}_g/\dot{m}_t$

μ_l	Liquid viscosity, kg/m-h
μ_g	Gas viscosity, kg/m-h
ρ_l	Liquid density, kg/m^3
ρ_g	Gas density, kg/m^3
θ	Inclination to the horizontal, degrees
α	Void fraction = $A_g/(A_g+A_l)$
ϕ_g	$\left[(\Delta P/\Delta L)_{TPF}/(\Delta P/\Delta L)_g\right]^{1/2}$
ϕ_l	$\left[(\Delta P/\Delta L)_{TPF}/(\Delta P/\Delta L)_l\right]^{1/2}$
ϕ_{gtt}	ϕ_g in the turbulent-turbulent flow mechanism
ϕ_{ltt}	ϕ_l in the turbulent-turbulent flow mechanism
$\eta_1, \eta_2, \eta_3, \eta_4, \eta_5$	refer to functions as have been used in the page 14.

LIST OF DIAGRAMS AND PHOTOGRAPHS

CHAPTER 1

1.1 Introduction

Two-phase flow is the simultaneous flow of a mixture of two-phases. If the phases are not of the same chemical composition, it is said to be a two-component two-phase flow. The flow of air-water mixtures falls in this category. Thus, the flow of steam-water will be termed as single component two-phase flow. The terms adiabatic and diabatic are introduced in two-phase flow in order to distinguish the case without heat transfer from that with heat transfer.

Two-phase flow occurs in boilers, condensers, refrigerators, natural gas pipe lines, air-lift pumps and nuclear reactors. However its occurence in nuclear reactors has attracted the attention of many workers recently. In order to design any of the above types of equipment, it is necessary to be able to predict the pressure drop, the void fraction, the density, the maximum flow rate, and heat transfer characteristics in pipes and ducts of various cross sections.

In a general sense, diabatic two-phase flow is a coupled thermodynamic problem. A single component two-phase flow in a vertical or horizontal conduit can never become fully developed. Furthermore, additional

complexities are introduced into two-phase flow phenomena by the hydrodynamic instabilities and the occasional thermodynamic non-equilibrium between the phases.

Owing to the inherent complexities of the physical process in two-phase flow, many variables are involved and therefore dimensional analysis yields very little simplification. In order to reduce a two-phase flow problem to tractable proportions, many simplified analytical and experimental studies have been conducted with some success.

All the mathematical models proposed by different investigators for the analysis and development of correlations for pressure drop, void fraction, flow patterns etc. of two-phase flow fall in one extreme or another and are thus approximate to the actual situation. Therefore, these models have been successfully used in correlating the experimental data only within certain limits of accuracy. However a good deal of empirical knowledge has been built up in this field. The total number of experimental measurements of two-phase pressure drop is currently well above 20,000, half of which have been obtained since 1959[18]. This continued accumulation of data demonstrates that this type of flow still lacks phenomenological understanding and thus forms a basis for further investigation.

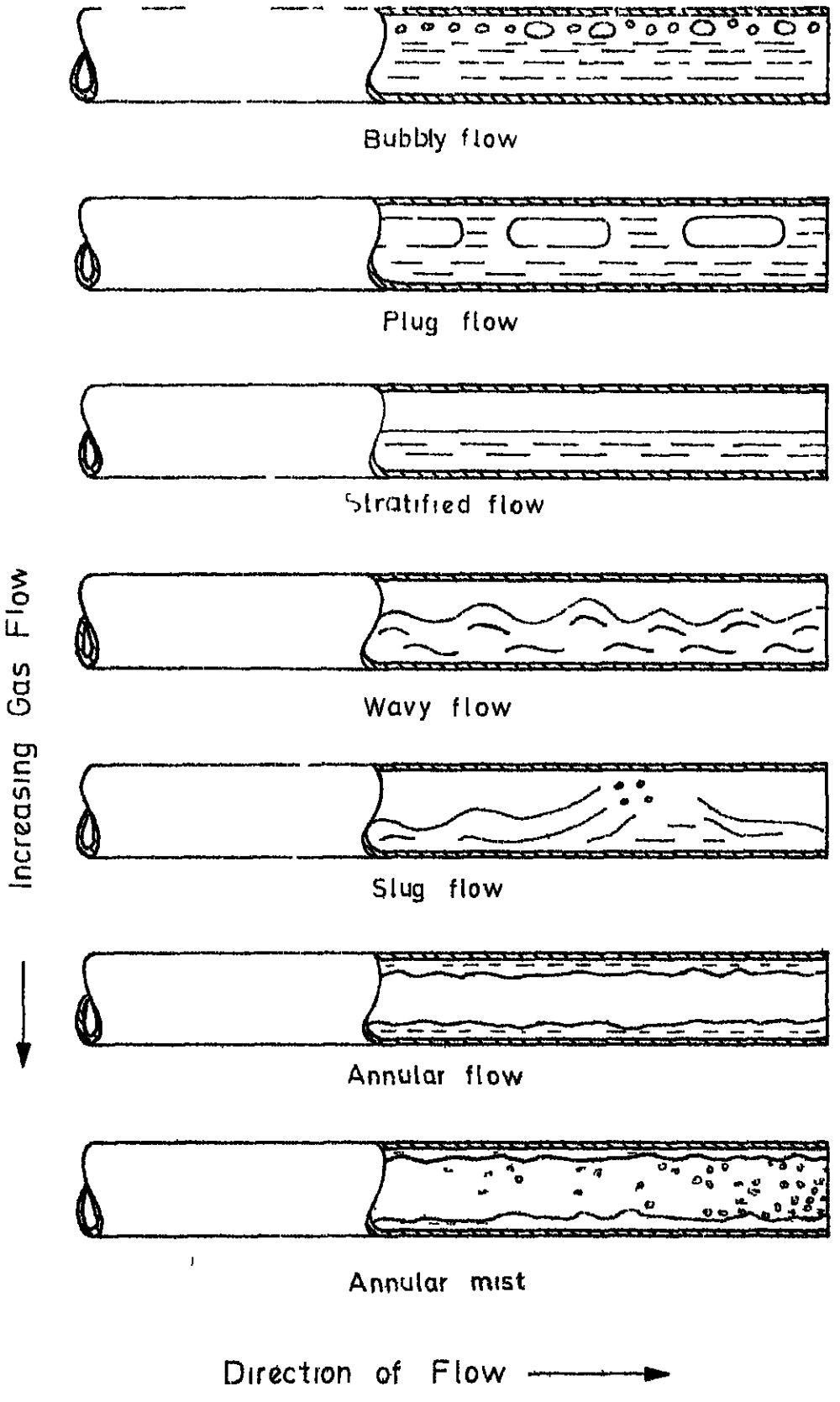

FIG 1 Schematic Diagram of the Flow Patterns

1.2 Review of Previous Work

The co-current flow of a gas and a liquid (air-water) through a horizontal pipe is characterised by a number of different flow patterns describing the structure of the flow. Figure 1 shows diagrammatically the various flow patterns as studied by Alves[4] who has described them as follows :

"Assume a horizontal pipe with liquid flowing so as to fill the pipe and consider the types of flow that occur as gas is added in increasing amount".

(i) Bubbly flow : Flow in which bubbles of gas move along the upper part of the pipe at approximately the same velocity as the liquid.

(ii) Plug flow : Flow in which alternate plugs of liquid and gas move along the upper part of the pipe.

(iii) Stratified flow : Flow in which the liquid flows along the bottom of the pipe and the gas flows above, over a smooth liquid-gas interface.

(iv) Wavy flow : Flow which is similar to stratified flow except that the gas moves at a higher velocity and the interface is disturbed by waves travelling in the direction of the flow.

(v) Slug flow : Flow in which a wave is picked up periodically by the more rapidly moving gas to form

a frothy slug which passes through the pipe at a much greater velocity than the average liquid velocity.

(vi) Annular flow : Flow in which the liquid forms a film around the inside wall of the pipe and the gas flows at high velocity as a central core.

(vii) Annular Mist or Dispersed or Spray flow : Flow in which most or nearly all of the liquid is entrained as spray by the gas.

Baker[5] has presented a generalised plot showing the boundaries of the various patterns as functions of the mass velocities of the gas and liquid phases. He has also introduced correction factors which are functions of the physical properties of the two phases in an attempt to generalise the plot, as most of the available data are for air-water systems at atmospheric pressure.

Two principal types of flow models have appeared in literature in the analysis of void fraction and pressure drop, viz., the Homogeneous Model*[12,13] and the slip Model [2,3,11,14].

*The present work has been confined to the annular flow regime so far as pressure drop measurement is concerned. Therefore, Homogeneous Model cannot be expected to predict results of reasonable accuracy as in annular flow two distinguishable phases exist. Hence a discussion of the Homogeneous Model is excluded.

Lockhart and Martinelli[3] in their "slip Model or separated Flow Model" presented a moderately successful correlation for two-phase two-component flows. The correlations (though originally developed for Annular flow only) are applicable for Wavy, Annular and Dispersed flow in a horizontal pipe around atmospheric pressure, and predict the pressure drops to within ± 60%[17]. The correlation of Lockhart and Martinelli is a widely accepted one and the experimental results of the present investigation will be compared with these predictions.

The basic postulates upon which the analysis of pressure drop is based are :

(i) Static pressure drop for the liquid phase must equal the static pressure drop for the gaseous phase regardless of the flow pattern, as long as appreciable radial static pressure differences do not exist.

(ii) The volume occupied by the liquid plus the volume occupied by the gas at any instant must equal the total volume of the pipe.

These postulates infer that flow patterns do not change along the tube length and thus 'slug flow' is excluded from consideration. Four types of flow mechanisms have been recognized depending upon whether the individual phases flowing alone in the pipe is

viscous or, turbulent. They are :

(i) Flow of both the liquid and the gas may be turbulent (t-t flow).

(ii) Flow of liquid may be viscous and flow of gas may be turbulent (v-t flow).

(iii) Flow of liquid may be turbulent and flow of gas viscous (t-v flow).

(iv) Flow of both the liquid and the gas may be viscous (v-v flow).

The region $1000 \prec Re \prec 2000$ is a transition region.

The expression for the two-phase friction pressure drop in terms of the single phase friction pressure drop of either component flowing alone is

$$\left(\frac{\Delta P}{\Delta L}\right)_{TPF} = \left(\frac{\Delta P}{\Delta L}\right)_{GPF} \phi_g^2$$

$$= \left(\frac{\Delta P}{\Delta L}\right)_{LPF} \phi_l^2$$

where ϕ is an empirical function of X defined as

$$X^2 = \left(\frac{dP}{dL}\right)_{LPF} / \left(\frac{dP}{dL}\right)_{GPF}$$

All the four types of flow have been dealt in (3). For turbulent gas flow and turbulent liquid flow,

$$X_{tt} = \left(\frac{\mu_l}{\mu_g}\right)^{0.1} \left(\frac{\rho_g}{\rho_l}\right)^{0.5} \left(\frac{1-x}{x}\right)^{0.9}$$

and ϕ_{gtt} and ϕ_{ltt} is related as

$$\phi_{ltt} = \phi_{gtt} / \left[X_{tt}^{(2-n)/2} \right]$$

where n varies between 0.2 and 0.25.

These results were later modified by Martinelli and Nelson[2] to the following expression for the two-phase pressure drop at high pressures :

$$\left(\frac{\Delta P}{\Delta L}\right)_{TPF} = \left(\frac{\Delta P}{\Delta L}\right)_{LO} (1-x)^{1.75} \phi_{ltt}^2$$

This was obtained as a result of the empirically determined relationship

$$\left(\frac{\Delta P}{\Delta L}\right)_{LPF} = \left(\frac{\Delta P}{\Delta L}\right)_{LO} \left(\frac{m_l}{m_t}\right)^{1.75}$$

$$= \left(\frac{\Delta P}{\Delta L}\right)_{LO} (1-x)^{1.75}$$

Chenoweth and Martin[6] in their investigations, have measured the pressure drops for a wide range of two-phase flow conditions in horizontal pipes. The tests were made in 1.5 and 3 inch pipes using air and water at pressures from atmospheric to 100 psia. The best agreement with Lockhart-Martinelli correlation is found for performance at atmospheric pressure. The largest deviations are for data taken at 100 psia in the 3 inch pipe. In this case, the predicted pressure drop is higher than that observed by a factor ranging from 1.4 to 2.5.

Hewitt et al[16] have, however, found that the Lockhart-Martinelli correlations do not adequately take into account the influence of liquid mass velocity and that the flow pattern certainly influences the values of the two-phase pressure gradient.

Dukler et al[18] have systematically compared the existing correlations of two-phase flow frictional pressure drop and void fraction. Out of about twenty five correlations for pressure drop that have appeared in literature, they compared against one another, five of the most widely used correlations. The Lockhart-Martinelli correlation, the oldest of the five tested, shows the best agreement with a set of carefully collected experimental data on pressure drop.

Levy[11] has postulated a "Momentum Exchange Model" on the basis that the exchange of momentum between the liquid and the vapor (whenever x, α, or ρ_l/ρ_g varies) tends to maintain the sum of frictional and head losses equal for the two-phases. Correlating the above in mathematical form he derived Bernoulli type momentum equations which reduce to the following expression for two-phase pressure drop,

$$\left(\frac{dP}{dL}\right)_{TPF} = \left(\frac{dP}{dL}\right)_{LO} \frac{(1-x)^{1.75}}{(1-\alpha)^2}$$

The above expression is independent of mass velocity (G) and the geometry of the channel (d_e). The correlation

has been found to agree well with experimental results in horizontal and vertical test sections (circular) with and without heat transfer at pressures from 12 to 2000 psia. The predictions are 20% below the values measured.

The modification, suggested by Marchaterre[14] to Levy's model, incorporates the mass velocity and diameter effect into pressure drop equations. Assuming that the liquid phase pressure drop can be expressed in terms of some apparent liquid friction factor f_l and equivalent pipe diameter $d_{e(l)}$, then,

$$\left(\frac{dP}{dL}\right)_{LPF} = - \frac{2f_l}{d_{e(l)}} \frac{G^2(1-x)^2}{\rho_l g_c (1-\alpha)^2}$$

and for single phase liquid flow,

$$\left(\frac{dP}{dL}\right)_{LO} = - \frac{f_{LO}}{d_e} \frac{G^2}{2\rho_l g_c}$$

Marchaterre obtained the empirical relation using Petrick's[7] data,

$$\frac{f_l}{d_{e(l)}} = (1-\alpha) \frac{f_{LO}}{d_e}$$

Then substitution gives,

$$\left(\frac{dP}{dL}\right)_{LPF} = \frac{(1-x)^2}{(1-\alpha)} \left(\frac{dP}{dL}\right)_{LO}$$

Now using Levy's postulate and the relation,

$$\left(\frac{dP}{dL}\right)_{TPF} = \left(\frac{dP}{dL}\right)_{GPF} + (1-\alpha) \left(\frac{dP}{dL}\right)_{LPF}$$

Marchaterre obtained the relation

$$\left(\frac{dP}{dL}\right)_{LPF} = \left(\frac{dP}{dL}\right)_{LO} \frac{(1-x)^2}{1-\alpha} + \frac{g(\rho_1 - \rho_g) f_1 \, d_e \, \text{Sin}\,\theta}{2 g_c \, f_{LO} \, G^2}$$

and for horizontal flow;

$$\left(\frac{dP}{dL}\right)_{TPF} = \left(\frac{dP}{dL}\right)_{LO} \frac{(1-x)^2}{1-\alpha}$$

According to Marchaterre the theoretical predictions will deviate considerably from experimental data if the flow pattern does not happen to be annular. Also, this formulation does not preclude the existence of mass flow rate effect in horizontal flow, since it is expected that changes in flow pattern can also cause changes in frictional pressure drop.

Muscettola's[19] comparison of the above results have been summarized as follows :

Levy's correlation shows a limited agreement for the range of variables considered, which can be attributed mainly to the fact that this correlation does not take into account a dependence on mass flow rate, and diverges as the quality approaches unity.

Martinelli and Nelson's correlation, which is not dependent on mass flow rate, shows a better agreement, however, the differences increase with an increase in the mass flow rate.

Marchaterre's correlation give a very poor agreement with the experimental results, due to its large dependence on the tube diameter.

Very few papers have been published on two-phase flow in bends and curved channels. Sekoguchi, K., et al[20] have correlated the total pressure drop due to bends using the parameters ϕ_1 and X, which are analogically introduced from the Lockhart-Martinelli parameters for a straight tube. They have exhibited the correlation between ϕ_1 and X using the ratio of R/d as a parameter. Only 90° bends of 18.02 and 25.70 mm diameter and R/d ratios of 5.02 and 2.36 were used in their experiments. Agreement between experiment and theory is reasonable.

The work of Boyce, B.E., et al[21] describes an experimental study of the flow patterns, liquid hold-ups, pressure gradients for the flow of air water mixtures in a series of helically coiled plastic tubes 1.25 inch diameter and D/d ratios varying from 9.6 to 96. The flow patterns observed for two-phase flow in helical coils are similar to those seen in horizontal two-phase flow, and occur in the same relative location on a flow pattern map. The Baker flow map, however, does not predict the flow pattern transitions seen in this study. At a given water flow rate, the air flow rate at which the transition from one flow regime to another takes place decreases with decreasing coil diameter. The pressure drop and hold-up data taken for these coils are adequately correlated by the Lockhart-Martinelli relationships. This is in agreement with the findings of other workers in helical coil. Detailed effect of liquid flow rate and flow

pattern are observed in the results when plotted using the Lockhart-Martinelli co-ordinates.

Paleyev, I.I., et al[23] investigated experimentally the motion of an air-water mixture at close-to-atmospheric pressure and room temperature in elbows (90°) with rectangular cross-section for the ratio of the duct height h to the turning radius R within the limits 0.045 to 0.86.

In these experiments they measured the total two-phase pressure drop in elbows. The two-phase flow pressure drop was considered as due to (i) the total friction losses, and (ii) the local losses caused by deformation of flow velocity fields in turns. Thus,

$$(\Delta P)_{TP} = (\Delta P)_{fr} + (\Delta P)_{turn}$$

$$= \bar{f}_{fr} \frac{l \bar{\rho} v_g^2}{d_e 2 g_c} + \bar{f}_{loc} \frac{\bar{\rho} v_g^2}{2 g_c}$$

where, $\bar{\rho} = \rho_g (1 + m_{sus}/m_g)$

In single-phase flow f_{loc} is a function of α, of R/h and of h/b. In two-phase flow $\bar{f}_{loc}$ is additionally a function of the flow variables. By analogy with single-phase flow the friction losses in the elbow are regarded as being the same as in a straight duct with the given initial phase flow rates.

The local resistance factor due to turning of the two-phase flow may be calculated from the following experimental expression

$$\bar{f}_{loc}/f_{loc} = 1 + 270\ Re_f^{0.38}\ Re_g^{-0.65}$$

This formula can be put in the form

$$\bar{f}_{loc} = \eta_1 (f_{loc}) \eta_2 (Re_g\ Re_l)$$

since the friction factor

$\bar{f}_{fr} = \eta_3 (Re_g\ Re_l)$ in two-phase flows, is a function of the same variables, it is possible to relate $\bar{f}_{loc}$ and $\bar{f}_{fr}$ by the expression

$$\bar{f}_{loc} = \eta_4 (f_{loc}) \eta_5 (\bar{f}_{fr})$$

$$= c\ f_{loc}\ \bar{f}_{fr} \quad \text{where} \quad c = 80$$

Thus, knowing the friction factor for two-phase flow in a straight duct and the local pressure drop factor for dry air, it is possible to calculate the total pressure losses for a two-phase flow in a curved duct.

$$(\Delta P)_{TP} = \bar{f}_{fr}\ \frac{\rho v_g^2}{2 g_c} \left(\frac{l}{d_e} + c\ f_{loc}\right)$$

Inspite of the large amount of literature in the area of two-phase flow, the information is still scarce for pressure drop data for annular and dispersedflow in 180° bends

which are practically encountered in design problems in connection with steam raising units, chemical reactors, boiling water reactors, evaporators, and condensers.

1.3 Scope of the Present Work

The present work consists of the study of adiabatic, isothermal flow of air-water in a series of bends (180°) with different radii of curvature and tube diameters. The object of the work is to make observations of the different flow patterns in two-phase flow and to measure pressure drop in two-phase annular flow in 180° bends, (set up in horizontal plane) as a function of air and water flow rates and curvature-to-tube diameter ratios (D/d).

The range of experimental variables covered is as follows :

Air flow rate : Ranging from 5 to 25 kg/h

Water flow rate: 22.62, 113.1, 226.2 and 339.3 kg/h

Temperature of air : 37 to 39°C

Temperature of water : 35 to 37°C

Pressure : 1 to 2 atm. absolute

Geometry of bends under study :

Test Section No.	Diameter of tube, d mm	Diameter of curvature, D mm	D/d
1	11.6	260, 200, 160, 100	22.41, 17.24 13.79, 8.62
2	16.2	260, 200 160, 100	16.04, 12.35 9.88, 6.18

In addition, the present work is intended to check whether some of the correlations proposed for annular flow, can be meaningfully extended to these flow conditions and also to compare the present results against Lockhart-Martinelli plot[3] and that of Sekoguchi et al[20].

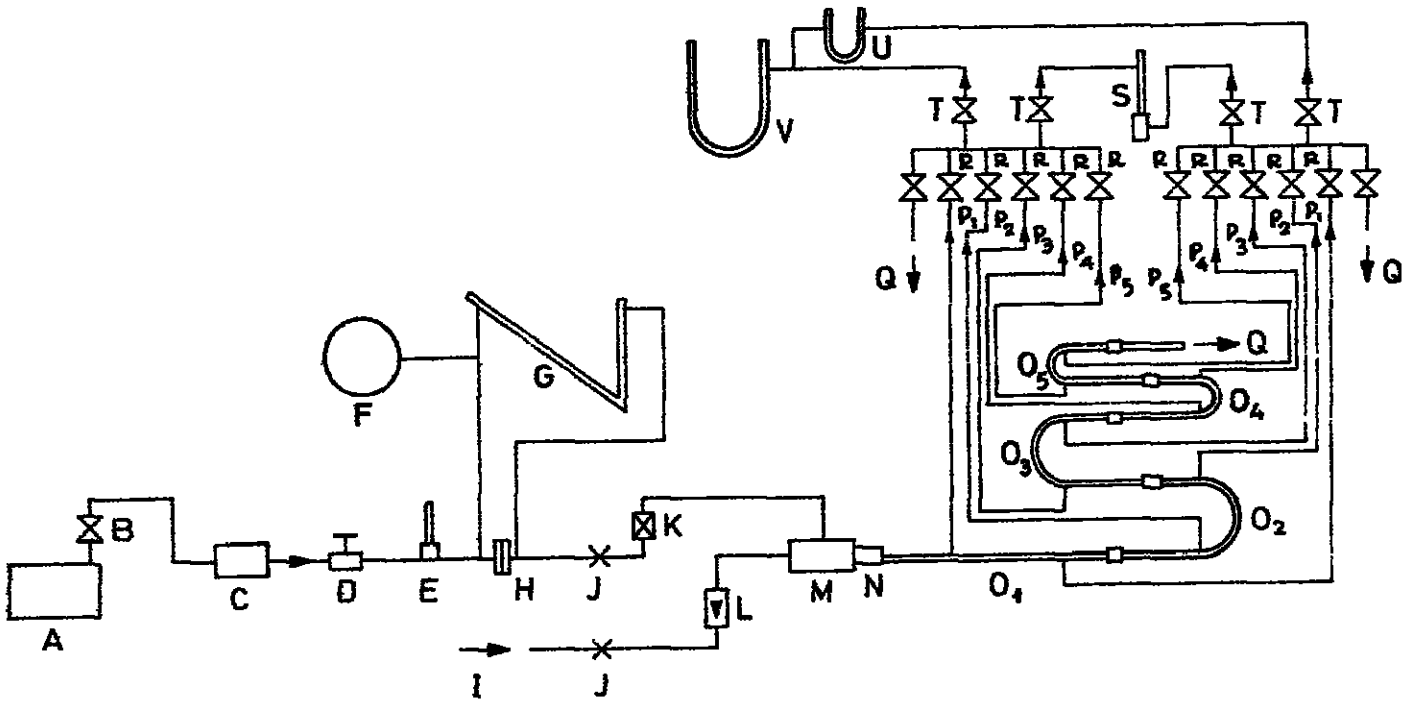

A Reciprocating compressor

B Valve

C Drying chamber

D Pressure regulator

E Mercury thermometer

F Pressure Gauge

G Inclined Manometer

H Orifice plate

I Water from supply mains

J Needle valve

K Non-return valve

L Rotameter

M Air-water mixing chamber

N Test section holder

O_t Straight test section

O_2 O_3 O_4 O_5 180 degree bend test sections

P_1 P_2 P_3 P_4 P_5 High pressure tappings

P_1 P_2 P_3 P_4 P_5 Low pressure tappings

Q To drain

R Pressure tapping selectors

S Liquid manometer

T Manometer selectors

U V Mercury Manometer

FIG. 2 SCHEMATIC DIAGRAM FOR TWO-PHASE (AIR-WATER) FLOW 'N BENDS

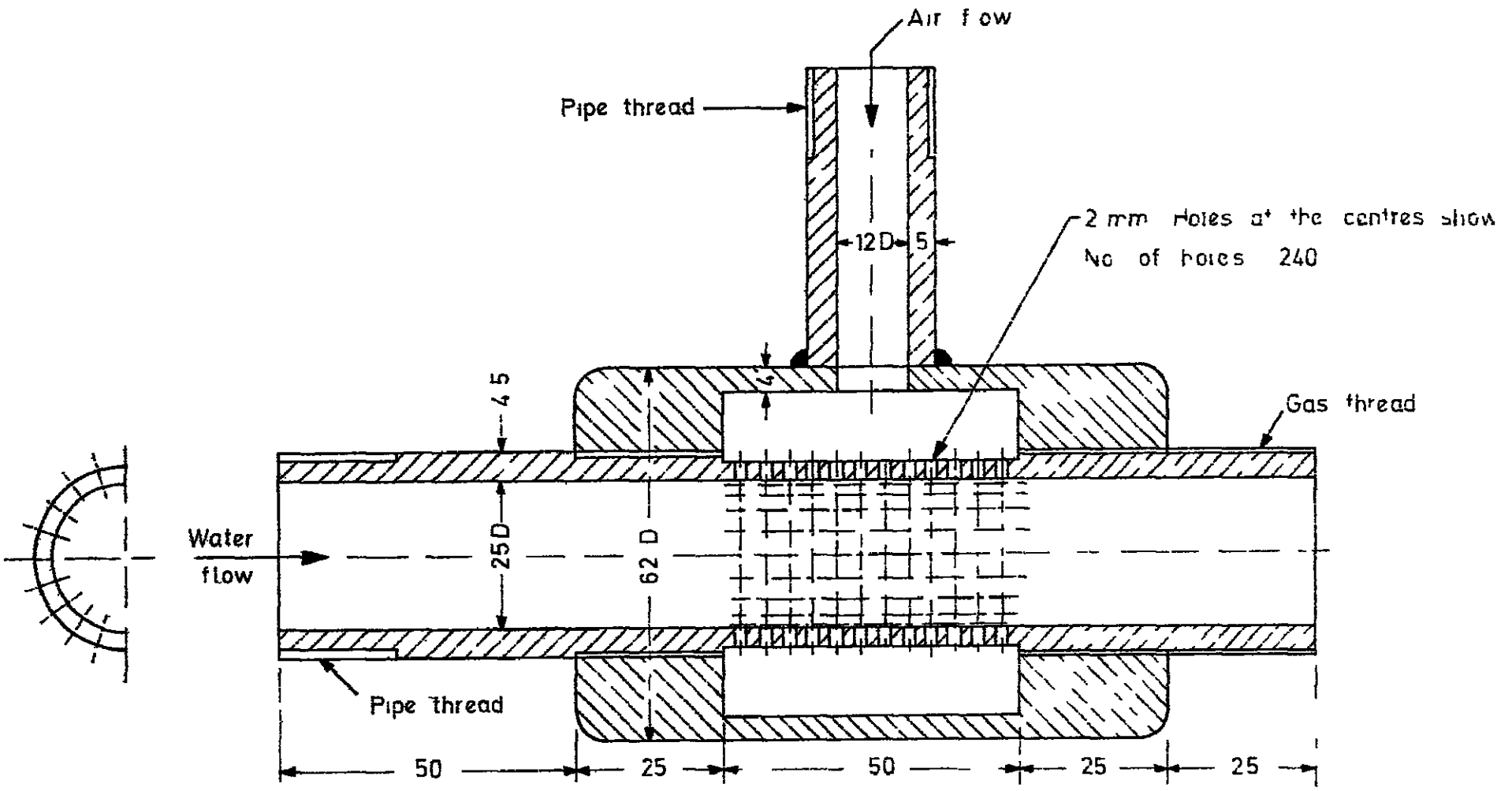

Sectional elevation

Dimensions are in mm

Scale Full size

FIG 3 MIXING CHAMBER

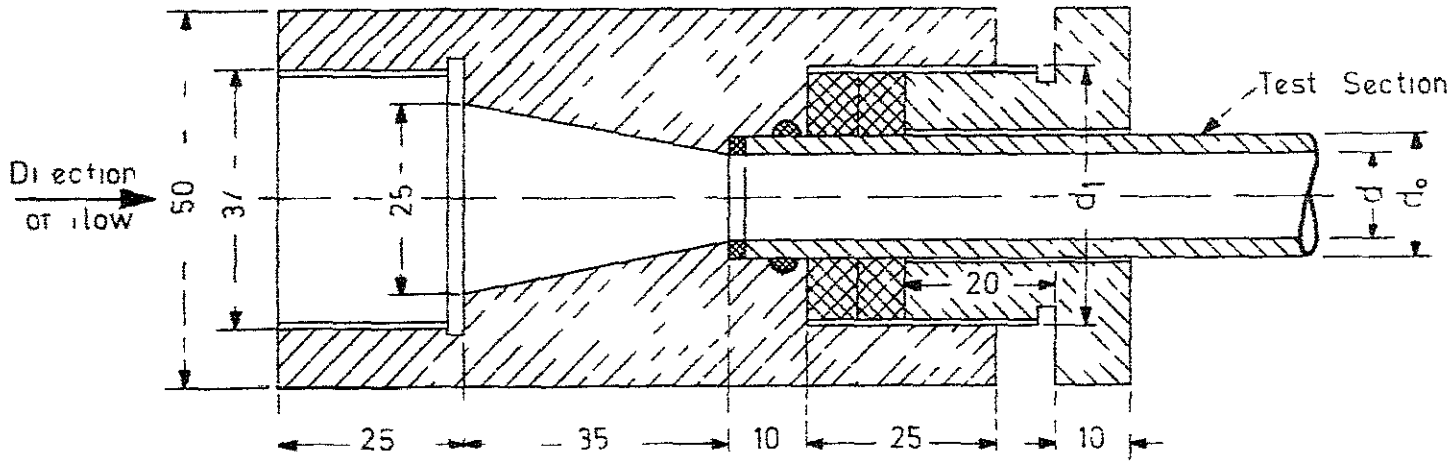

Dimensions are in mm

Scale Full Size

Sectional Elevation

FIG 4 TEST SECTION HOLDER

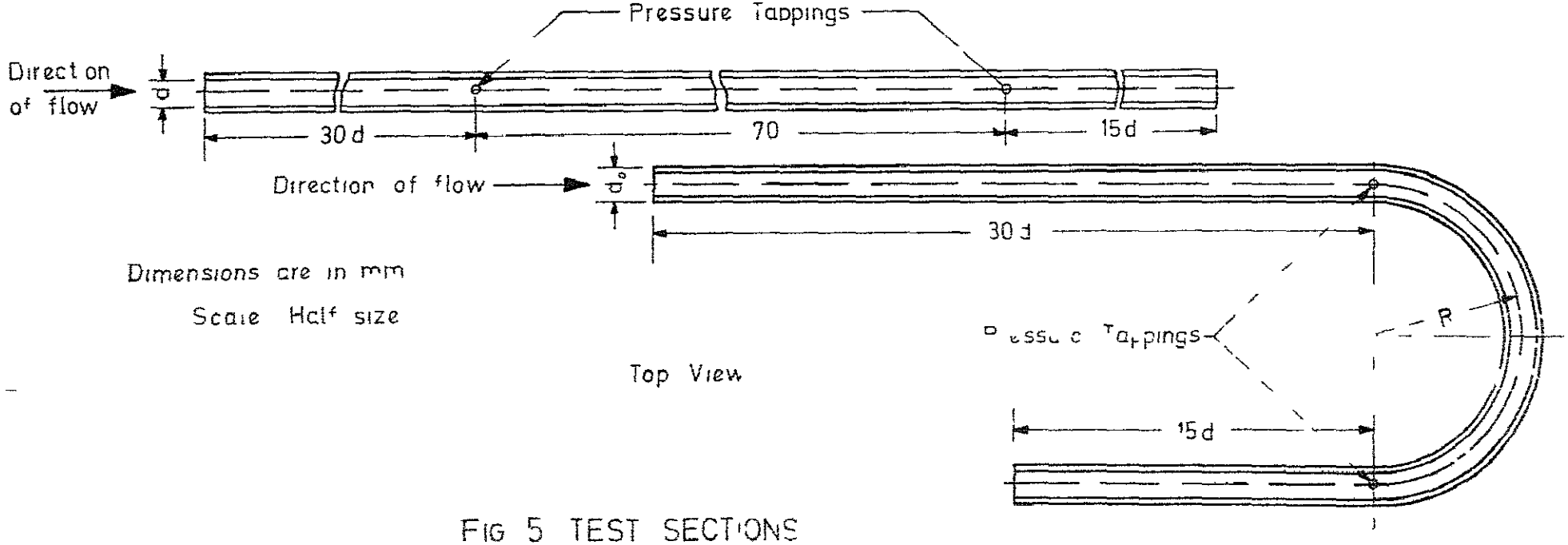

Dimensions are in mm

Scale Half size

Top View

FIG 5 TEST SECTIONS

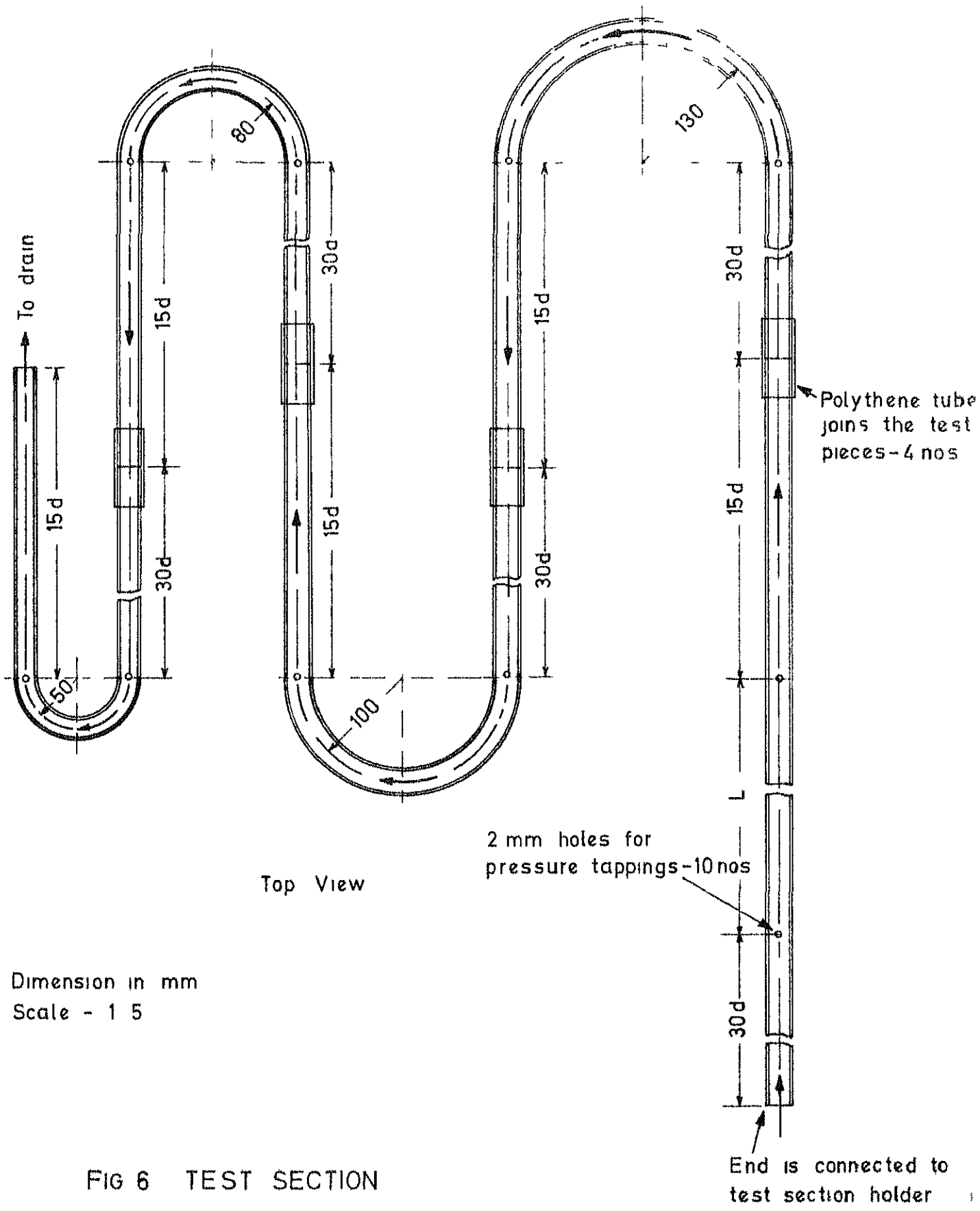

Top View

Dimension in mm
Scale - 1 5

FIG 6 TEST SECTION

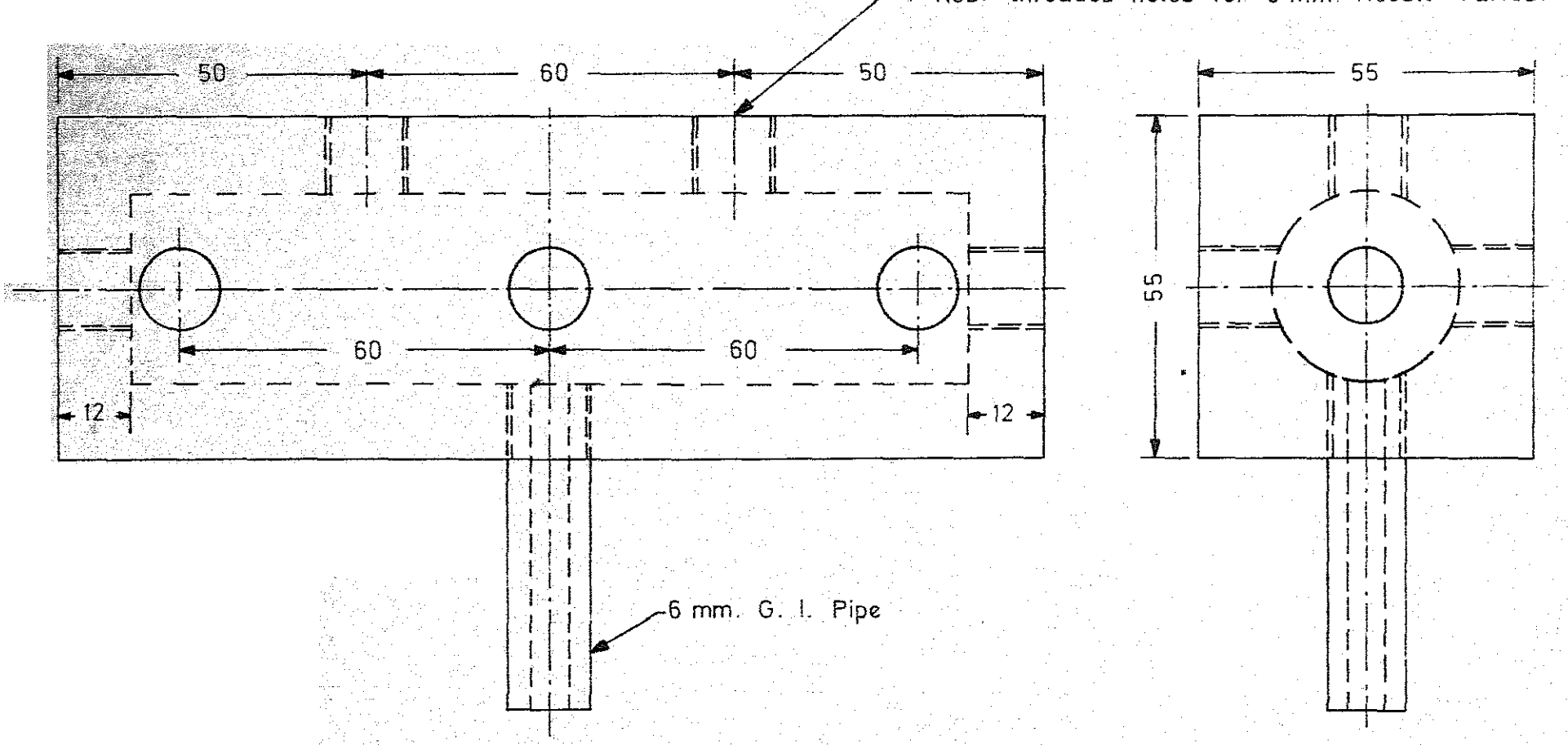

FIG. 7. PRESSURE HEADER

Dimension in mm.
Scale: Full Size
Nos : Two

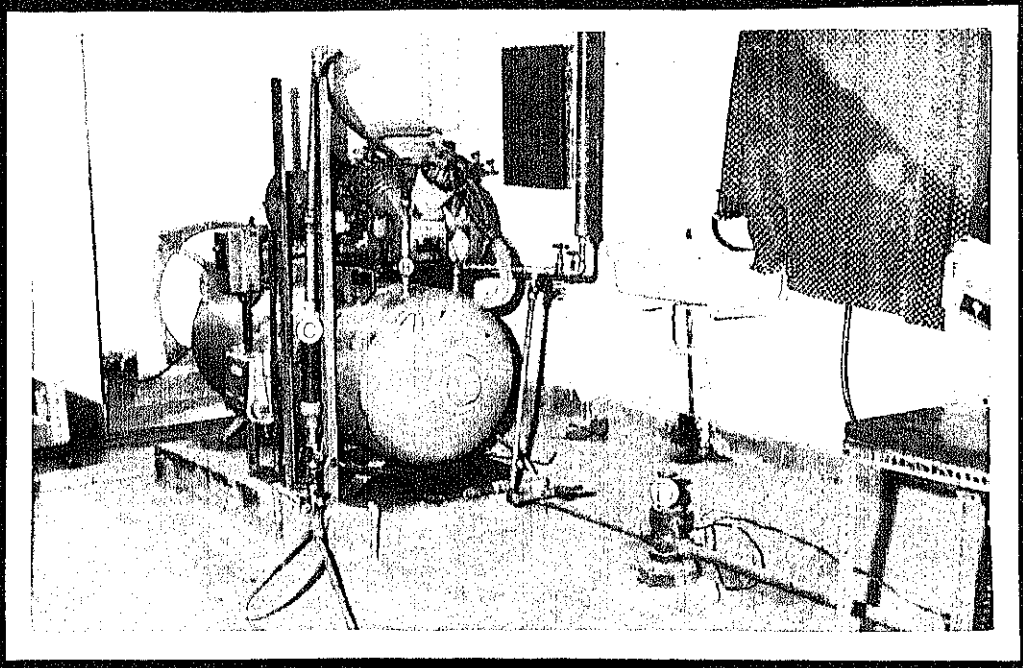

FIG.8 (a)

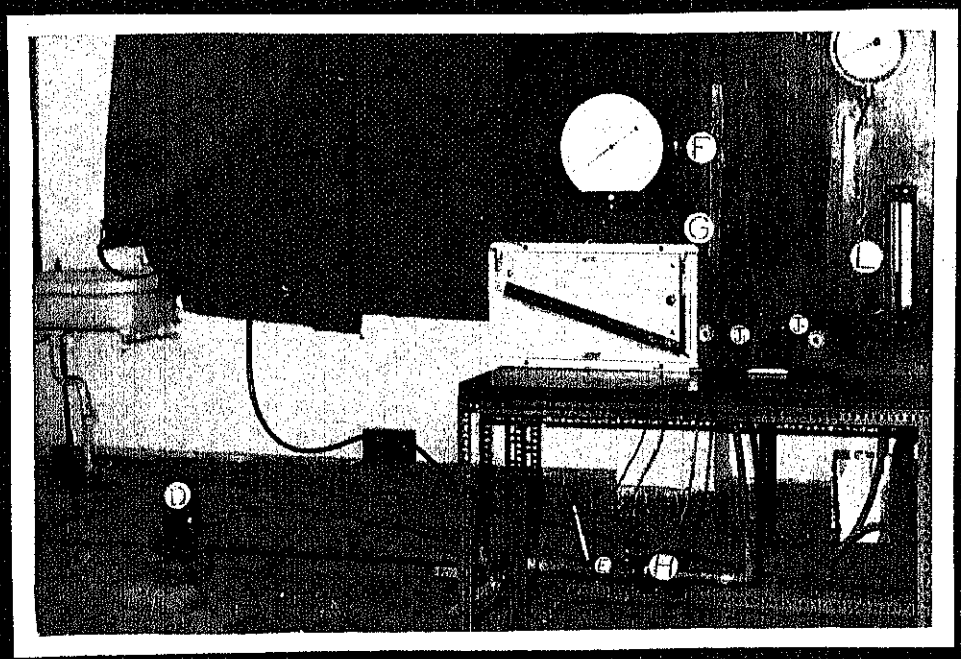

FIG.8 (b)

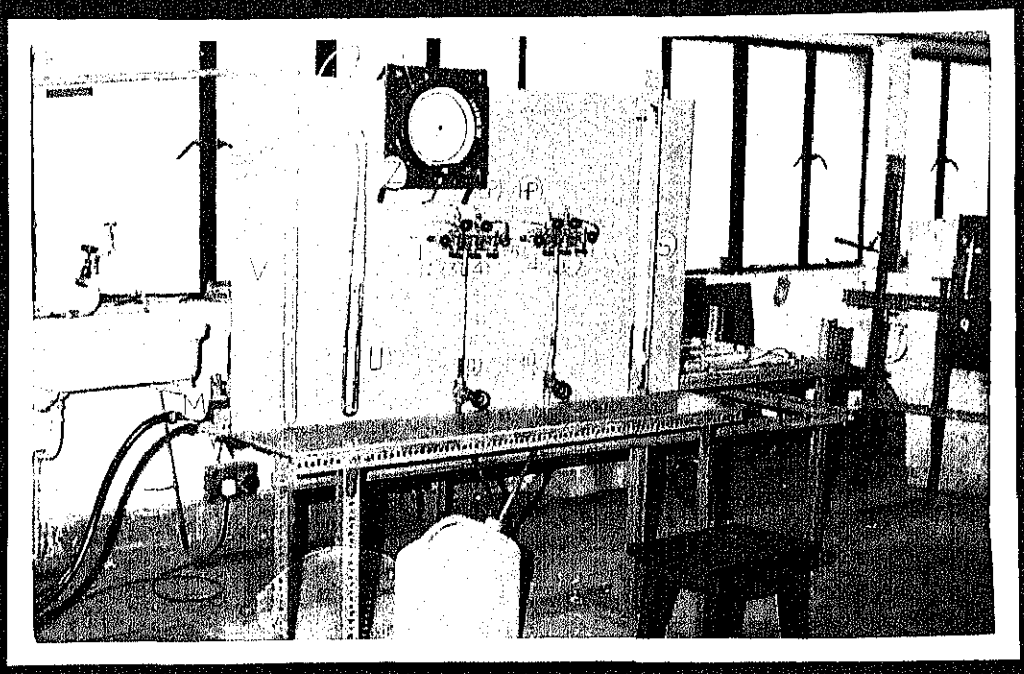

FIG. 8(c)

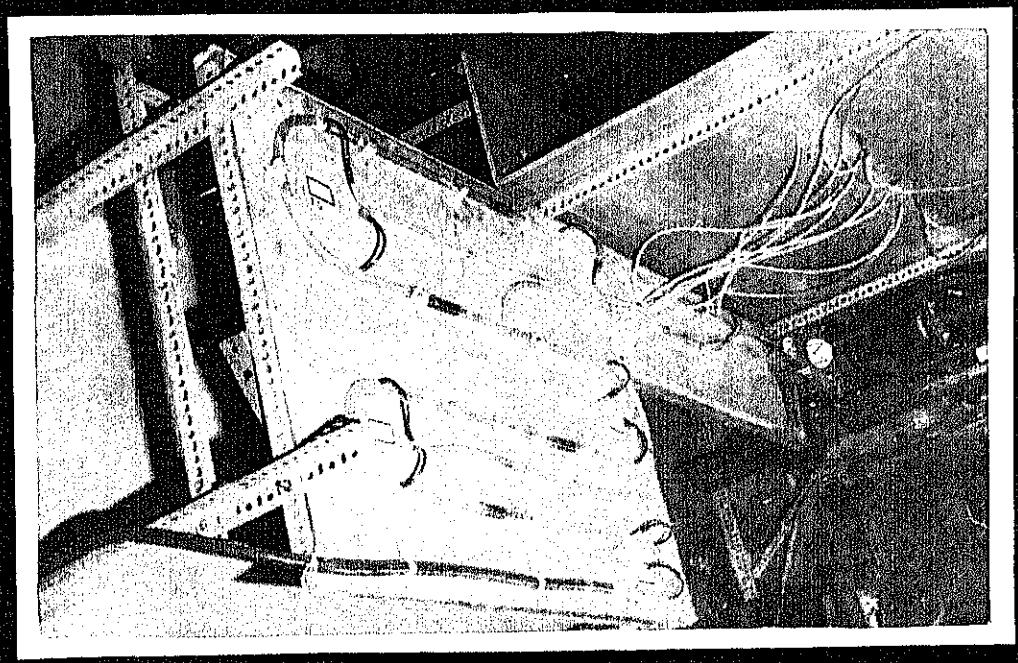

FIG. 9

CHAPTER 2

2.1 Apparatus

A schematic diagram of the apparatus for the present study is shown in Fig. 2. The apparatus has been fabricated so as to accommodate a change in the test-section when necessary. Photographic views of the apparatus are shown in Figs. 8 and 9.

Air delivered from a two-stage reciprocating compressor, is dried by passing through a chamber containing silica-gel. It is then passed in succession through a pressure regulating device, orifice plate, flow control valve and nonreturn valve, after which, it flows into the air-water mixing chamber.

Water from main supply is passed, via a rotameter and flow control valve, to the mixing chamber. All the controlling valves are of the needle type.

The air-water mixture from the mixer flows through the test section holder, to the test section (containing one straight piece and four 180° bends of different curvatures but all of the same diameter) and finally to a drain.

Details of the important parts of the apparatus are given below.

(a) Mixing Chamber :

The purpose of the mixing chamber is to mix the phases (air-water) thoroughly in proper proportion, and to discharge the mixture at equilibrium condition into the test sections. Figure 3 shows a detailed drawing of the mixing chamber, which is similar to that used by Sagar et al[21].

The unit consists of two parts : the inner part is the 25 mm (G.I.) pipe having 240 (2 mm size) drilled holes on its circumference over a length of 50 mm. The outer part is in the form of a socket, threaded on the pipe forming an air tight enclosed annulus with the pipe wall covering the full length with holes. Water flows through the inner pipe. Air flows first into the annulus and then enters the G.I. pipe through the 2 mm holes. It now mixes with water in the main tube, forming the required two-phase mixture.

(b) Test Sections (Figs. 5, 6 and 9) :

Pyrex glass tubes of two diameters 11.6 and 16.2 mm were used for the test sections. Out of the same diameter tube, one straight section and four 180° bends of diameters 100, 160, 200, and 260 mm were made. Thus two sets (five each) of test-section were made using two different diameters. The bends were shaped using wooden patterns which had been pre-formed. In these operations the error introduced due to the deformation in both diameter and the curvature were within $\pm$7% and 3% respectively.

In each test piece two holes (2 mm diameter each) were made using a hot Tungsten wire, at positions shown in Figs. 5 and 6. These holes were used to connect the test section to manometers to measure the pressures and pressure drops in the straight section (of 700 mm length) as well as bent sections. Entry and exit lengths for each test piece were provided as 30d and 15d respectively as suggested in (15). The recommendation of Sekoguchi, K., et al[20] for the entry and the exit lengths also fall well within the above values for the range of flow conditions considered in the present work. Further all the test pieces with the same diameter, were connected to make one test-section (as shown in Fig.6) using a straight section first and then bends in a decreasing order of radii of curvature. In a test section, two test pieces were joined giving a perfect contact using fixing material and a piece of polythene tube having the diameter sufficient to hold the test section (shown in Fig.6).

Connections to manometers were made by using 6 mm polythene tubes joined to the glass with the help of fixing materials so as to maintain the 2 mm hole unobstructed. Thus in each test section there were ten pressure tappings.

The test sections were connected to the mixing chamber using a specially designed test section holder, a detailed drawing of which is provided in Fig. 4.

2.2 Instrumentation

The instrumentation was sufficient to measure the flow rate, (both air and water) temperatures and pressures at various points in the flow.

For measuring the water flow rate, a rotameter of capacity 0 to 2 gpm (Brooks make with least count 0.05) was connected in the water line, before the mixing chamber. The rotameter was calibrated by collecting and measuring the amount of water flowing through the rotameter for a known time. No difference in the calibration was noted.

For air flow measurement, an orifice meter was fabricated* and used as specified in the ASME Power Test Code[9] and also[10]. The diameters of the pipe and the orifice were 38.89 mm and 11.97 mm respectively. The measured air flow rate was found to range from 5 to 25 kg/h. The flow is turbulent in the test section at all the measured flows. The error involved in this measurement is within $\pm$ 8%[10].

The expression giving the air flow rate through the orifice meter is

$$\dot{m}_g = 8160.19K \left[\bar{h}_w P/T\right]^{1/2} \text{ kg/h.}$$

The constant K is related to flow Reynolds number as given by Table 1 below[9].

---

* The orificemeter was designed and used by Mr. J. Tewary for his M.Tech. thesis project. Author is grateful to him for sparing the same.

TABLE 1

Dependence of K on Reynolds Number

Re	K	Re	K
500	0.6405	10,000	0.6064
1000	0.6276	15,000	0.6045
2000	0.6186	20,000	0.6036
3000	0.6145	25,000	0.6028
4000	0.6121	50,000	0.6010
5000	0.6105	10^5	0.5997
6000	0.6093	10^6	0.5976
8000	0.6076		

A pressure regulating valve (make M/s. Drayton Greaven Ltd.) was connected in the air supply line before the orifice meter in order to provide different flow rates at constant pressure (shown in Fig. 8(a) and (b)). The constant pressure thus maintained upstream of the orifice plate was 20 psig.

The temperatures of the air, water, and air-water mixture were measured with the help of mercury-in-glass thermometers (least count being 0.1°F).

The static pressure and pressure drop in the orifice meter were measured respectively with a pressure gauge (Heise make with least count 0.1 psi) and an

inclined manometer (Dwyer make using red oil of specific gravity 0.825) with a least count of 0.02 inch of water (shown in Fig.8(b)).

The pressure headers (Figs. 7 and 8(c)), one for the high pressure side and one for the low pressure side were used in order to facilitate the handling of the ten pressure tappings by a single manometer and also to drain the water from the pressure connections. Out of ten pressure tappings in each test section, five high pressure tappings were connected to the high pressure header and the low pressure tappings to the low pressure header, (as shown in Fig.2) using one selector valve of needle type in each line so that only two could be selected at a time for the manometer reading. On the other hand, the headers were connected to manometers through valves. For the measurement of static pressure at the entry to each test piece a U-tube mercury manometer (least count : 0.1 in. of Hg) was used and for the measurement of pressure drop in the test pieces, a vertical manometer with red oil (specific gravity 0.824; least count 0.1 in. of water) was used. Both the manometers are Dwyer make.

The pressure connections, upto a certain length starting from the test section, were maintained horizontally (shown in Fig. 9) as the test section and the header were

mounted at a higher level. The manometer connections were made at the top of the header. All these helped in the accuracy of the measurement and also to avoid the contamination of water with red oil in the manometer.

2.3 Test Procedure

The procedure followed was essentially the same for each test section. Before taking any reading it was assured that there was no leakage in any section of the set up starting from the pressure regulating valve to the drainage. In this connection the procedure followed was to raise the pressure in the pipe line upto certain level (say 30 psig). Then the respective valves were closed and the readings of the gauges and the manometers were observed. If there was any drop in the reading, then the detection of the leakage in the corresponding section was carried out by putting concentrated soap solution in the joints, and the joints tightened until no more leakage was noticed. In some sections this procedure was repeated several times. Finally the system was assumed to be completely free from leakage by the indication of constant readings in the manometer and the gauges for a whole day.

Care was taken to drain the water in the pressure connections from time to time during the tests to eliminate the chances of its collection in the vertical portion of

the polethene connections for pressure measurement. Thus errors that would arise in the manometer reading due to the presence of water column in the vertical portion of the connections was avoided and at the same time the chances of water mixing with manometer liquid was eliminated.

The tests for single-phase flow were performed first. The compressor was run to gain a certain pressure, before opening its outlet valve. After opening the flow controlling valve, the pressure regulating valve was adjusted to give a particular working static pressure in the orifice plate (20 psig was chosen). Then a series of runs were carried out over the full air flow range available to enable the single-phase friction factor for each test section to be calculated. The readings at any air flow rate consisted of static pressure, and pressure drop at the orifice plate and five static pressure and five pressure drop readings in the test section in addition to those for temperatures. The readings were repeated for other flow rates covering the range.

A set of readings were taken to calculate the pressure drop for water alone, flowing in the test section. The flow rates of water used were those necessary in the two-phase flow experiment. In this case a rotameter was used to measure the flow rate instead of orifice plate as was used for air flow measurement.

For two-phase flow pattern studies, at selected water flow rates (0.1, 0.5, 1.0, and 1.5 gpm) a range of air flow rates were used, in order to obtain desired flow structures. Thus at a particular water flow rate, all the flow patterns were studied (as shown in Fig. 1) by increasing the air flow rate from a minimum so as to start with bubbly flow.

The procedure for the pressure drop test consisted of setting up the desired air flow rate for a selected water flow rate so as to get fully developed annular flow in the whole test section. When the conditions were steady, a full set of readings of air flow rate, water flow rate, pressures and temperatures were taken. Manometer readings at the different test sections were taken one after another using the proper selector valves in the headers. The sequence followed was to run a range of air flows at a number of selected water flow rates maintaining the flow pattern in the test section fixed.

The reproducibility of readings was checked by taking a number of repeated observations with each test section, in both single-and two-phase flow after a few days interval. The flow rates were maintained the same for each repetition.

CHAPTER 3

DATA REDUCTION

3.1 Single-phase Pressure Drop

Plots of pressure gradient vs. flow rate were prepared for both components of flow separately for the bends and the straight portion. The single-phase friction factor for each bend as well as the straight portion was calculated by using the expression

$$f = \left[\Delta P/(\rho v^2/2g_c)\ (d/l)\right]$$

where l for a curved pipe was $(\pi/2)d$. And the Reynolds number was calculated from the expression :

$$Re = vd\rho/\mu = 4\dot{m}/(\mu\pi d)$$

where $v = \dot{m}/\left[(\pi/4)d^2\rho\right]$ the variables $\dot{m}$, v, ρ and μ take the suffices g and l for the air and water flow respectively.

The friction factor for Laminar flow in normal straight smooth pipe is given by

$$f_s = 64/Re$$

The Nikuradse-Von Karman equation correlates the data for turbulent flow in a straight smooth pipe as

$$1/\sqrt{f_s} = 2.0\ 10g_{10}(Re\sqrt{f_s})-0.8$$

White[1] has developed an expression for the friction factor for laminar flow in curved channels. For laminar flow, the increase in pressure drop in the curved pipe over that in a straight pipe is expressed in terms of the dimensionless grouping

$$De = \left[Re(d/D)^{0.5}\right]$$

The values of the factor by which the resistance of a straight pipe at the same Reynolds number must be multiplied is given by

$$f_c/f_s = \left[1.0 \left\{1.0 - (11.6)^{0.45}/De\right\}^{2.22}\right]^{-1.0}$$

where De is defined as above.

The transition from laminar to turbulent flow in a curved pipe occurs at a higher Reynolds number than for a straight pipe and is given by

$$(Re)_{trans} = 2300\left[1.0 + 8.6\ (d/D)^{0.45}\right]$$

The transition Reynolds number increases as the d/D ratio increases.

With turbulent flow in a curved pipe, the expression for the friction factor is given by Ito[3] as

$$f_c = 0.304\ (Re)^{-0.25} + 0.029\ (d/D)^{0.5}$$

for $0.034 \leqslant Re\ (d/D)^2 \leqslant 300$

3.2 Two-phase Pressure Drop

The measured total pressure gradient is regarded as the sum of three components : frictional, accelerational and gravitational. Thus,

$$\left(\frac{dP}{dL}\right)_{TP} = \left(\frac{dP}{dL}\right)_{TPF} + \left(\frac{dP}{dL}\right)_{TPA} + \left(\frac{dP}{dL}\right)_{TPG}$$

In order to correlate the frictional pressure gradient, the measured value has to be corrected for the accelerational and gravitational head.

In the present work the acceleration pressure gradient, $\left(\frac{dP}{dL}\right)_{TPA}$ is zero since (i) there is no change of phase and (ii) the test section of constant cross section is used. The contribution of the centrifugal force to acceleration gradient in the axial direction is zero (which can be seen from Navier-Stokes equation for single phase flow). Its contribution in the radial direction has not been considered in the present work since the diameter of the tube is small in comparison with its length. Nevertheless the frictional pressure drop in a curved tube is greater than in a straight tube of the same length because of cross flow that has been observed at bends even in single-phase flow. The gravitational head $\left(\frac{dP}{dL}\right)_{TPG}$ or static head pressure gradient is zero as test sections were put horizontally.

The compressibility effect of air due to pressure change is neglected as the present work is confined to very low pressures.

Thus the frictional pressure gradient is equal to the measured total pressure gradient, i.e.

$$\left(\frac{dP}{dL}\right)_{TP} = \left(\frac{dP}{dL}\right)_{TPF}$$

The frictional pressure gradient values have been correlated in terms of the dimensionless parameters X, ϕ_g, and ϕ_l as proposed by Lockhart-Martinelli[3]

$$X^2 = \left(\frac{dP}{dL}\right)_{LPF} \Big/ \left(\frac{dP}{dL}\right)_{GPF}$$

$$\phi_l^2 = \left(\frac{dP}{dL}\right)_{TPF} \Big/ \left(\frac{dP}{dL}\right)_{LPF}$$

$$\phi_g^2 = \left(\frac{dP}{dL}\right)_{TPF} \Big/ \left(\frac{dP}{dL}\right)_{GPF}$$

The value of $\left(\frac{dP}{dL}\right)_{TPF}$ for two-phase flow and that of $\left(\frac{dP}{dL}\right)_{LPF}$ and $\left(\frac{dP}{dL}\right)_{GPF}$ for single-phase flow are taken from the test data.

CHAPTER 4

4.1 Results and Discussion

(a) Flow Regime Test -

In these tests different flow patterns, corresponding to those shown in Fig. 1 were identified. However bubbly flow occurred for a very small range of air flow rates corresponding to each water flow rate. No clear stratified flow was observed in the studies. Though slugs of water were present in it, their frequency was very low. The wavy flow pattern was contaminated with a spray of water forming a wavy spray type of flow pattern similar to that observed by Boyce et al[21] in their investigation. At low flow rates of water the annular flow was quite distinct as compared with that of high flow rate. In the later case the gaseous core was mixed with mist. This was probably due to the type of mixing chamber used in the experiment.

Visual observations revealed that the transition from one type of flow to another did not occur simultaneously in all the bends and the straight portions of the test section. That means a flow condition may undergo transition only in a certain length of the test section containing one or even more bends and straight section but not in the whole of the section. At a particular

water flow rate, the air flow rate at which transition occurs decreases with increase in curvature, the tube diameter remaining constant, since centrifugal action is inversely proportional to the radius of curvature. For a particular curvature and water flow rate, the transition occurs at lower flow rate of air as tube diameter decreases. Also for fixed curvature and diameter of tube, the transition occurs at lower flow rate of air as water flow rate increases. In a curved pipe, the flow is also affected due to the centrifugal force arising out of changes in the flow direction. This causes the movement of bubbles, plugs, and slugs faster in the bends with higher curvature than in lower curvature. At the same time eddies are formed due to the variable static pressure over the tube cross section of the bends. The existence of eddies in the cross-section increases the flow of liquid from the inward to the outward elbow surface.

Figure 10 shows annular flow in 180°-bend (D/d = 13.9 and d = 11.6 mm). The photograph was taken from the top. It is seen that the liquid layer on the outer surface of the bend is thicker than that at the inner surface. And also the movement of the gas core is faster in the curved section than in the straight.

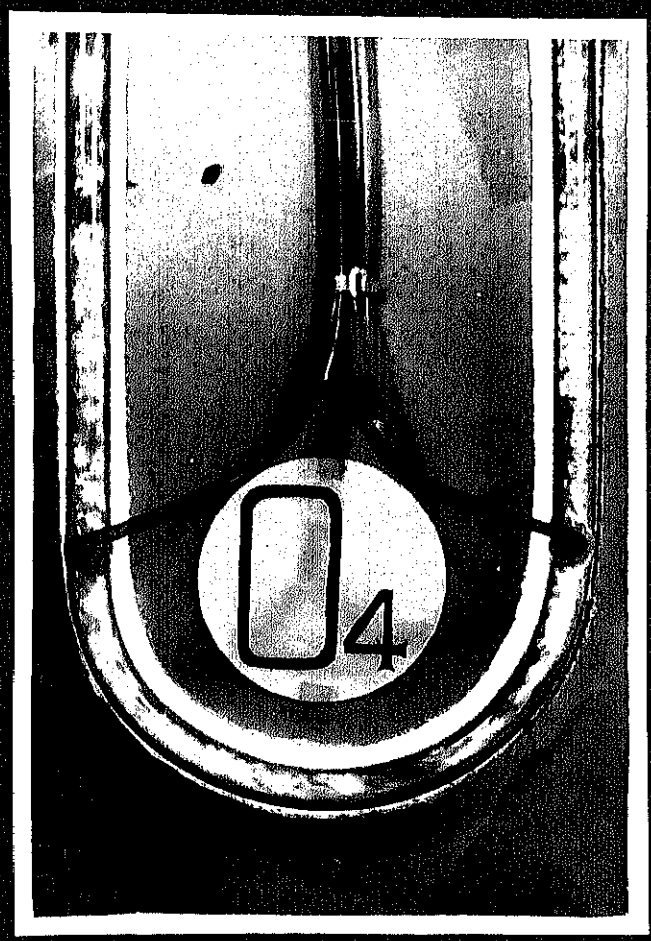

FIG. 10

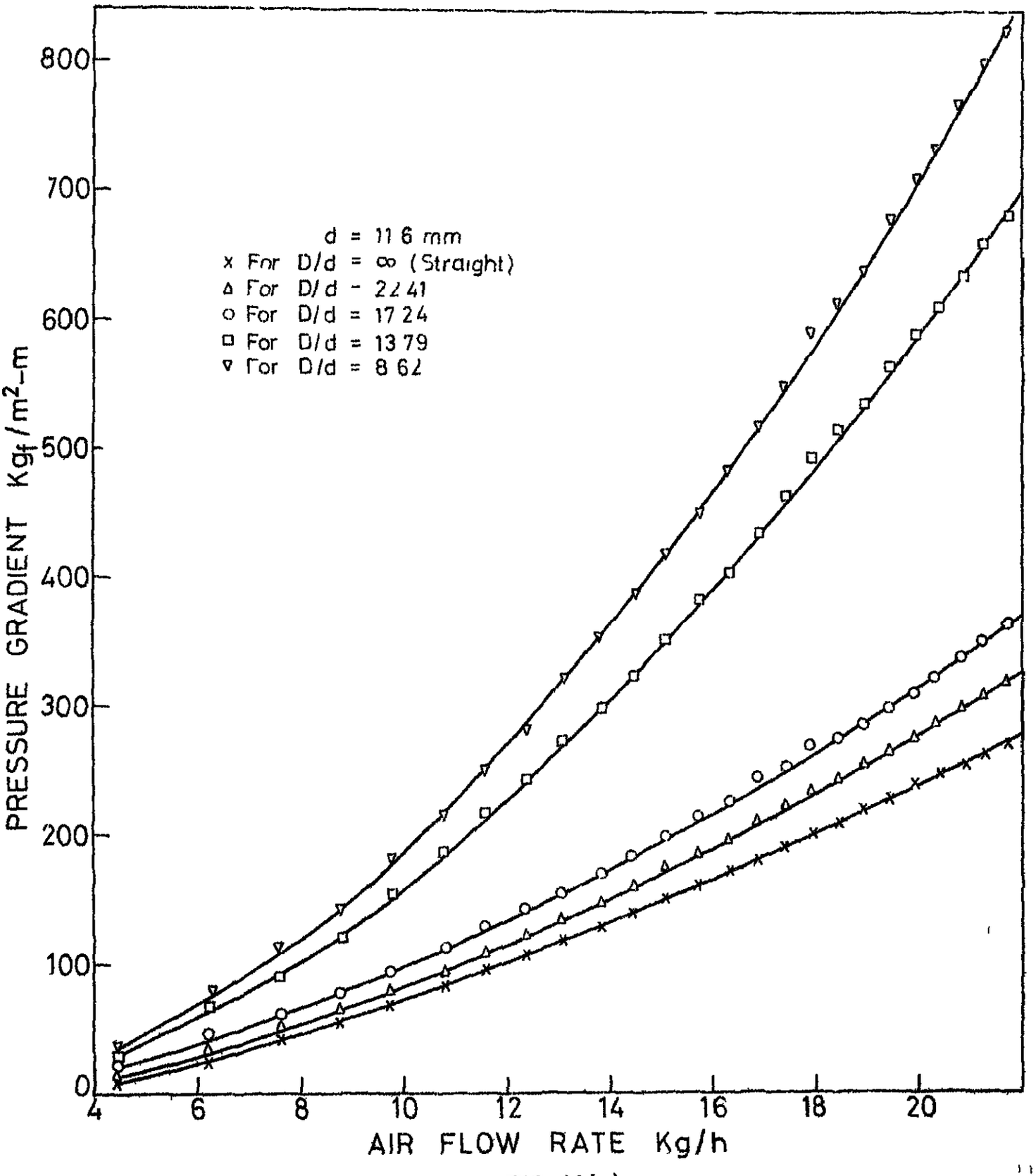
d = 11 6 mm
x For D/d = ∞ (Straight)
Δ For D/d = 22 41
○ For D/d = 17 24
□ For D/d = 13 79
▽ For D/d = 8 62
PRESSURE GRADIENT Kgf/m²-m
AIR FLOW RATE Kg/h
0
100
200
300
400
500
600
700
800
4
6
8
10
12
14
16
18
20

FIG 11(a)

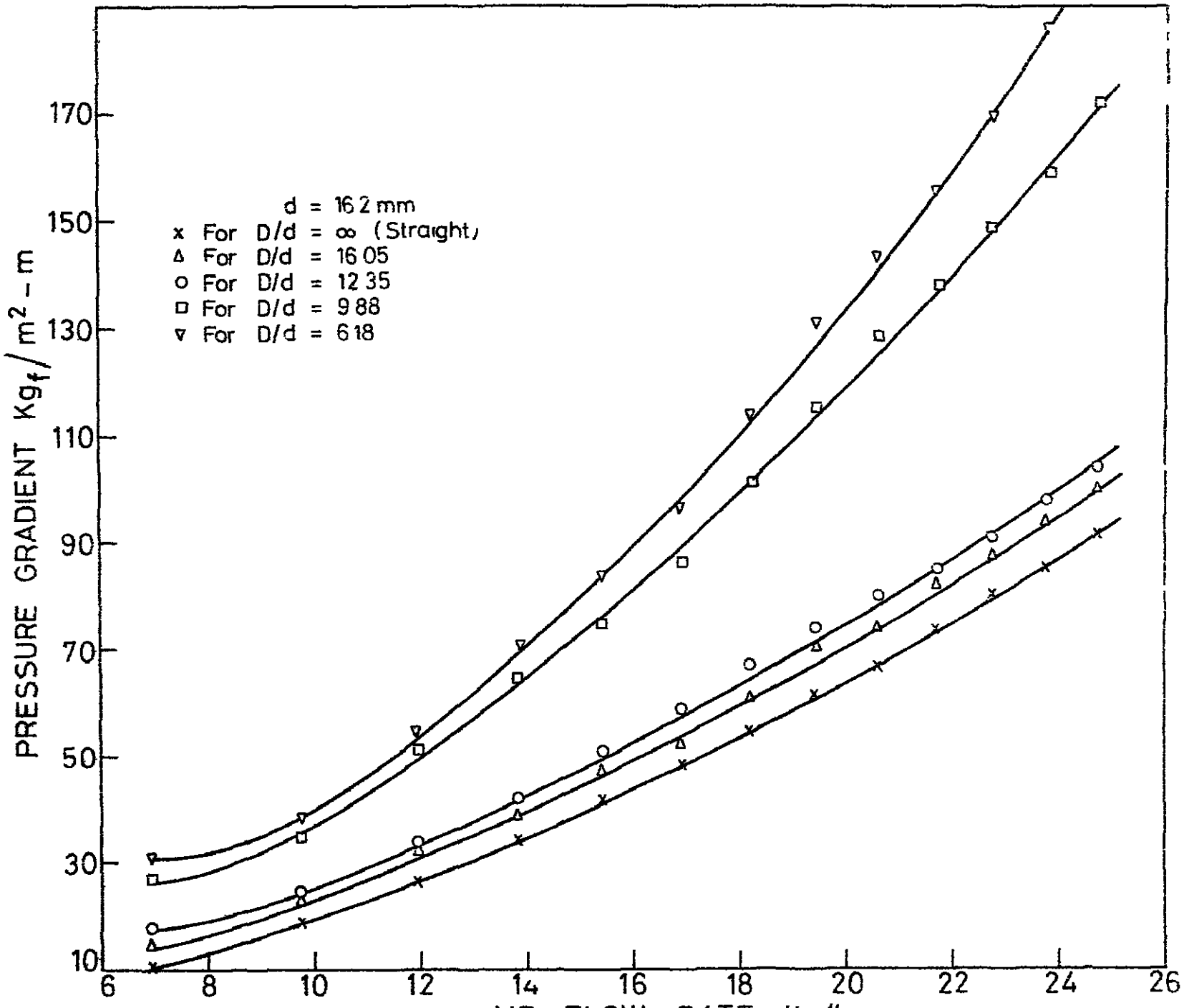
d = 16.2 mm
x For D/d = ∞ (Straight)
Δ For D/d = 16.05
o For D/d = 12.35
□ For D/d = 9.88
▽ For D/d = 6.18
PRESSURE GRADIENT Kgf/m² - m
AIR FLOW RATE Kg/h
10
30
50
70
90
110
130
150
170
6
8
10
12
14
16
18
20
22
24
26

FIG. 11(b)

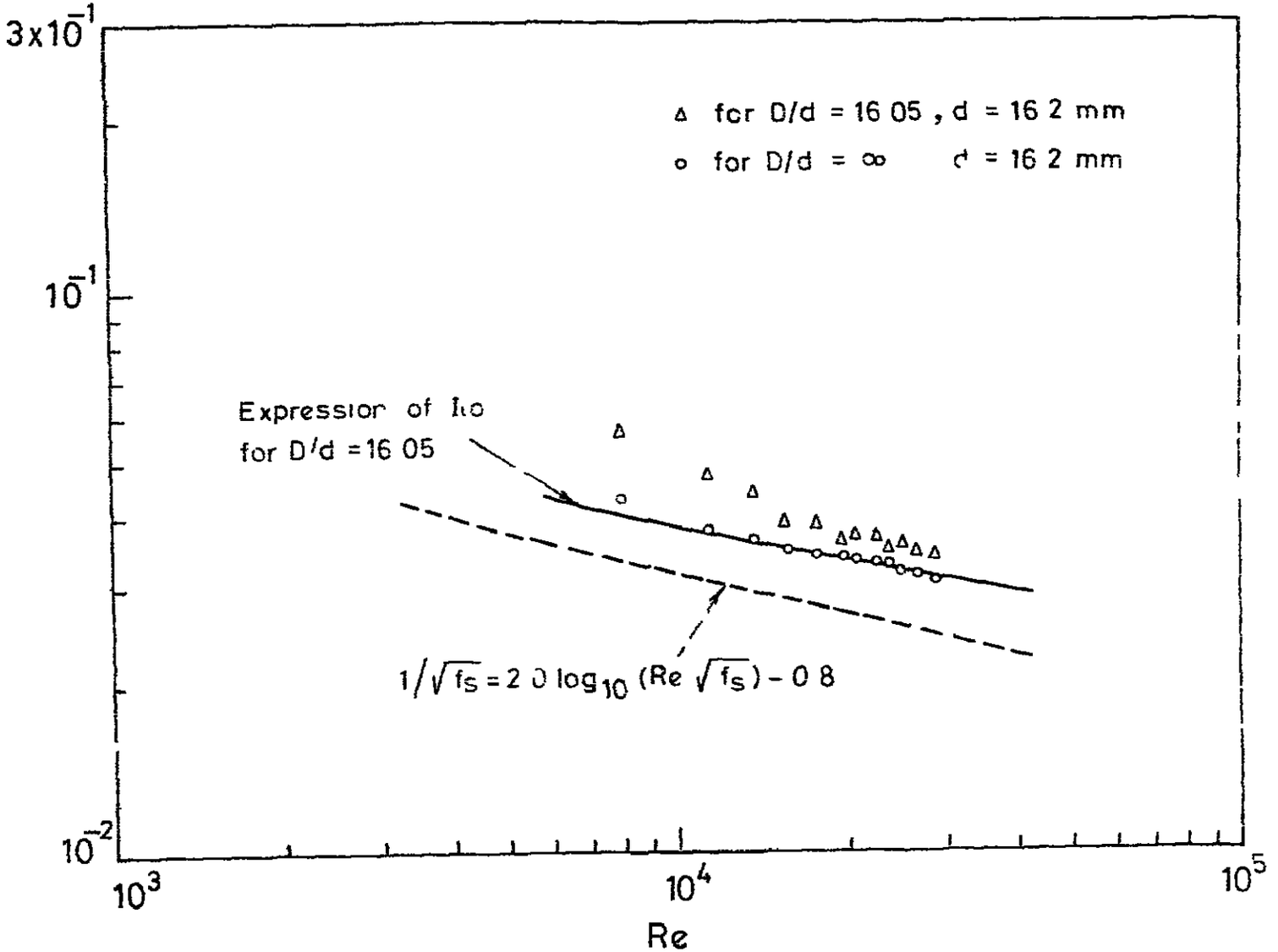
3x10⁻¹
10⁻¹
10⁻²
10³
10⁴
10⁵
Re
Δ for D/d = 16 05 , d = 16 2 mm
o for D/d = ∞ d = 16 2 mm
Expression of I.o
for D/d = 16 05
1/√fs = 2 0 log10 (Re √fs) - 0 8

FIG 12

(b) Single-phase Pressure Drop -

The plot of pressure gradient vs air flow rate has been shown in the Fig 11(a) for straight tubes as well as for D/d ratios 22 41, 17 24, 13 79 and 8 62 for d=11 6mm It is found as expected that with increasing radius of curvature of the bend, the pressure gradient shifts towards that of straight tube This is due to a decrease in centrifugal effects with increasing radius of the bend The slope of all the pressure gradient curves increase with increase of air flow rate Figure 11(b) represents a similar plot for a test section with d = 16 2 mm and D/d = ∞ , 16 05, 12 35, 9 88 and 6 11 The difference between these two plots is only in the value of pressure gradient which is expected to be less in case of higher diameter tube

The theoretical and experimental values for friction factors for various Reynolds numbers for a straight tube and a bend are shown in Fig 12 The experimental results for bends are higher by 10 to 30% than theoretical, since the tubes are not hydraulically smooth and commercial glass tubes are not perfectly circular Secondly, there may be some error (about + 5%) in the air flow measured with the orifice plate[10] The effect of this error on friction factor and Reynolds number has been illustrated in the next section viz the error analysis. The results

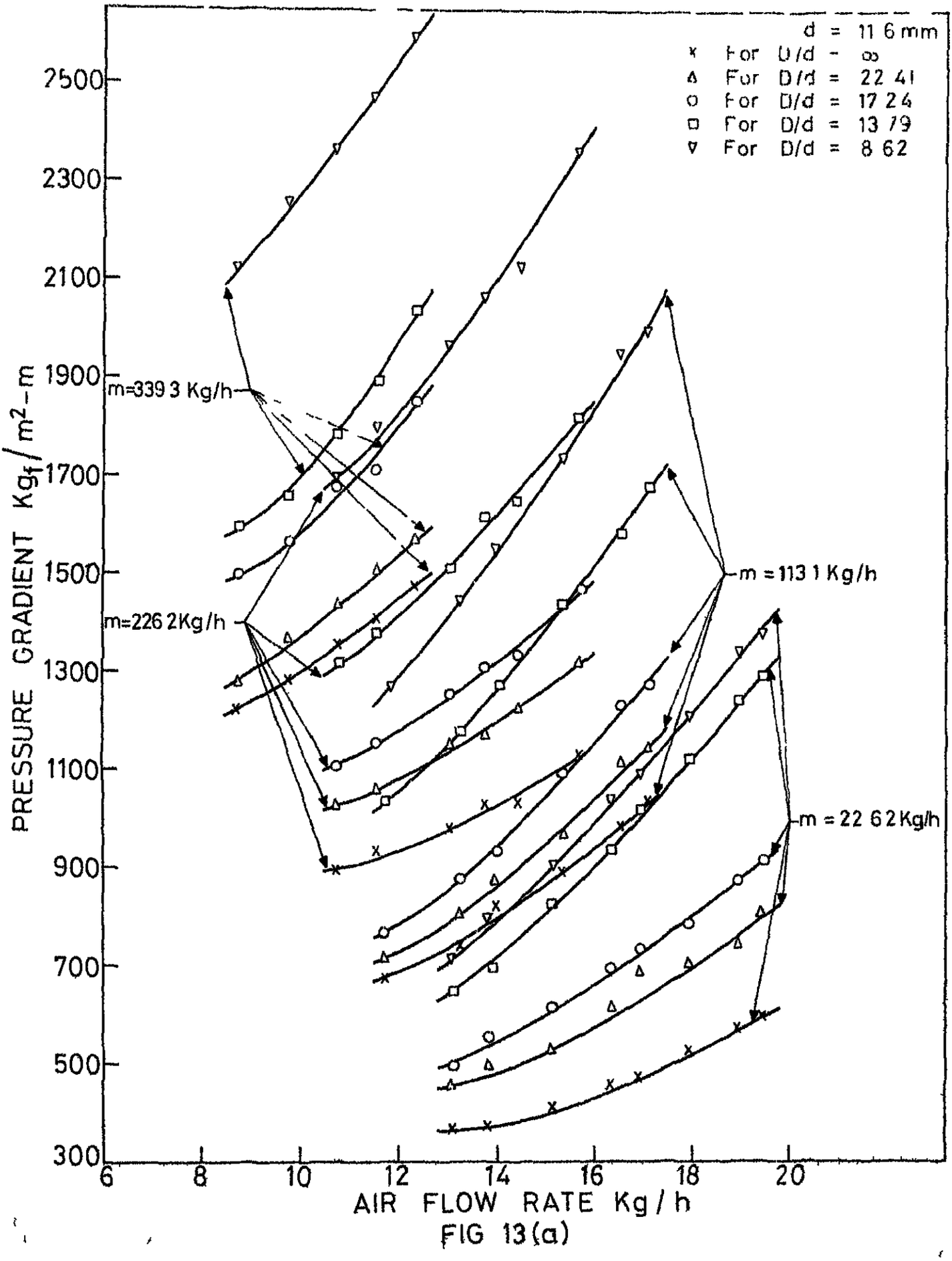
d = 11 6 mm
x For D/d = ∞
Δ For D/d = 22 41
o For D/d = 17 24
□ For D/d = 13 79
▽ For D/d = 8 62
m=339 3 Kg/h
m=226 2Kg/h
m = 113 1 Kg/h
m = 22 62Kg/h
PRESSURE GRADIENT Kgf/m²-m
2500
2300
2100
1900
1700
1500
1300
1100
900
700
500
300
6
8
10
12
14
16
18
20
AIR FLOW RATE Kg / h

FIG 13(a)

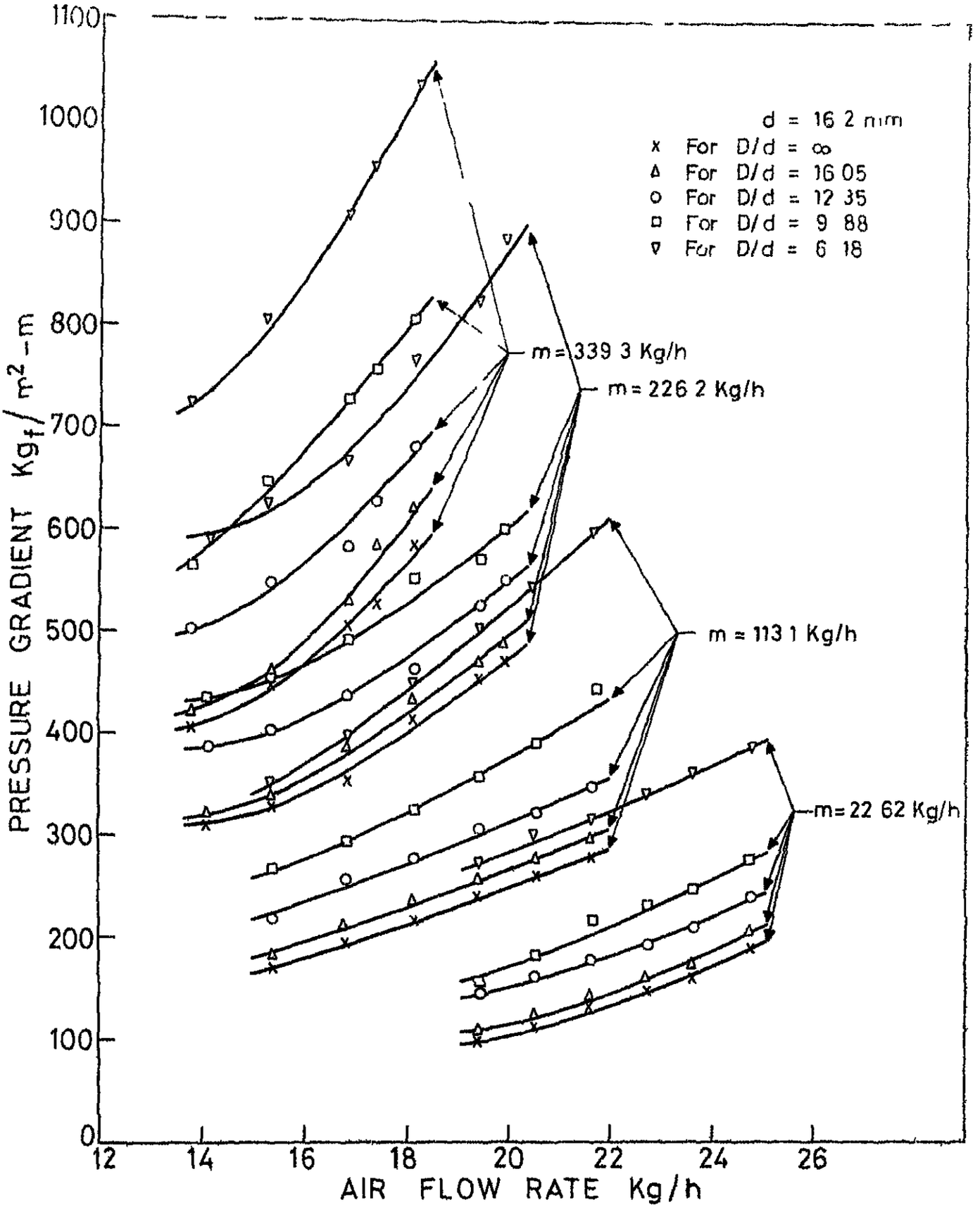
d = 16 2 mm
x For D/d = ∞
Δ For D/d = 16 05
o For D/d = 12 35
□ For D/d = 9 88
▽ For D/d = 6 18
m = 339 3 Kg/h
m = 226 2 Kg/h
m = 113 1 Kg/h
m = 22 62 Kg/h
PRESSURE GRADIENT Kgf/m2-m
AIR FLOW RATE Kg/h
0
100
200
300
400
500
600
700
800
900
1000
1100
12
14
16
18
20
22
24
26

FIG 13 (b)

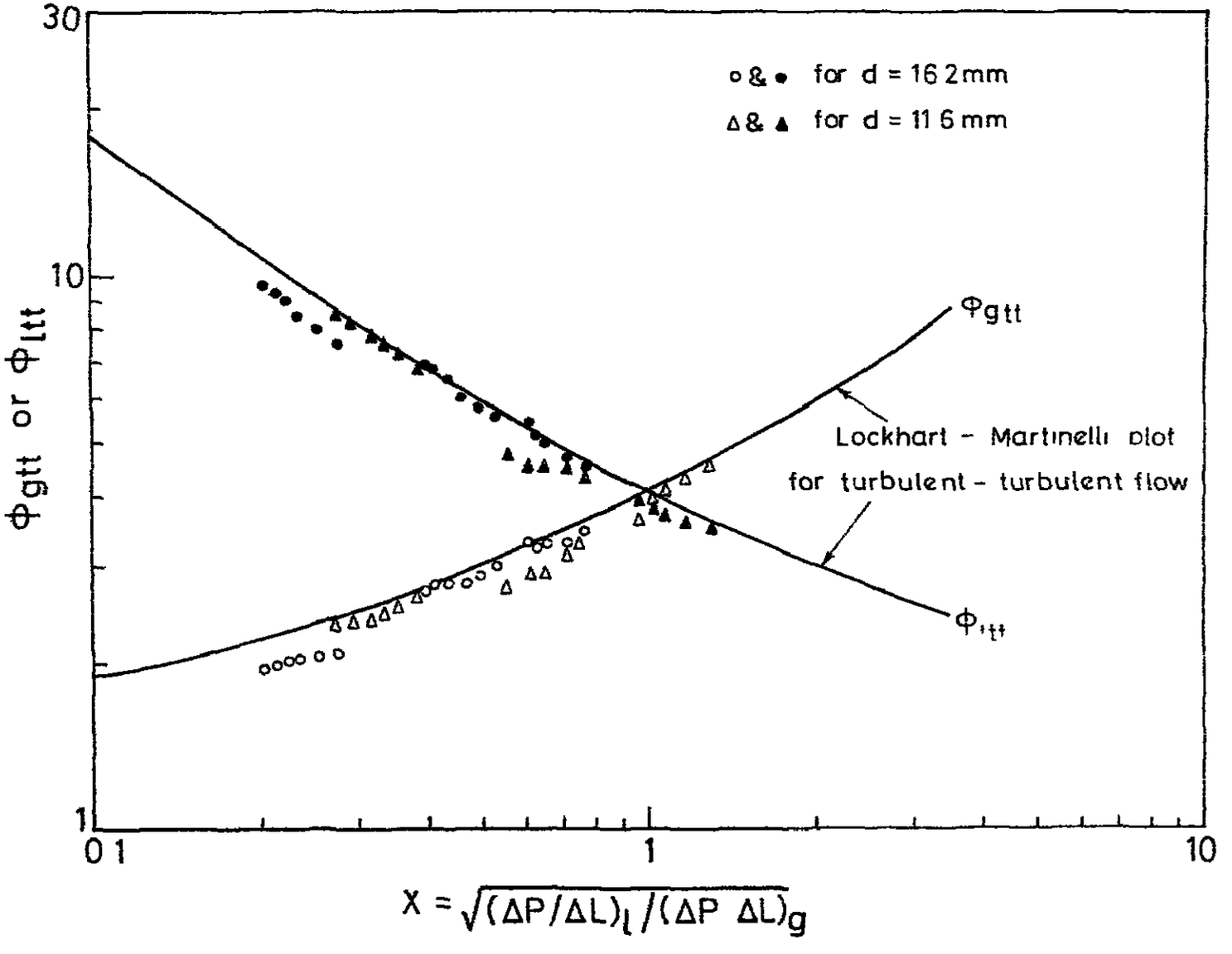
30
10
1
0 1
1
10
o & • for d = 16 2mm
Δ & ▲ for d = 11 6 mm
Φgtt
Lockhart - Martinelli plot
for turbulent - turbulent flow
Φltt
Φgtt or Φltt
X = √(ΔP/ΔL)l /(ΔP ΔL)g

FIG 14

for the straight tube are also higher than the data predicted through Von Karman equation by 25%. This difference is equivalent to a relative roughness (ϵ/d) value of 0.003 at Re = 3×10^4 for a straight pipe. The results obtained for the friction factor are summarized in Table 2. Although most of the experimental results have been found to be higher than the theoretical values, a few are lower than the theoretical values by about 10-15%.

(c) Two-phase Pressure Drop -

The results of two-phase pressure drop measurements are given only for annular flow in Figs. 13(a) and (b), where the measured pressure gradient has been plotted against the air flow rate with water flow rate and D/d ratio as parameters. The slopes of pressure gradient curves increase with the increase of water flow rate for a particular D/d ratio.

On Fig. 14, the correlating lines originally recommended by Lockhart and Martinelli[3] for straight horizontal pipes for turbulent-turbulent flow along with the present work for straight tubes for diameters 11.6 and 16.2 mm. are shown. It is observed that the present experimental values fall within 18% below the Lockhart-Martinelli plot. The results indicate that data for each liquid flow rate lie on a separate line with little scatter. This

TABLE 2

Summary of friction factor-Reynolds number relationship for the bends and straight tube

Re	D/d = ∞ d=11 6 mm	D/d=22.41 d=11 6 mm	D/d=17.24 d=11 6 mm	D/d=13.79 d=11 6 mm	D/d=8.62 d = 11 6 mm
9893	0 0301	0 0314	0.0296	0.055°	0 0733
13922	0 0284	0.0307	0.0264	0.0563	0.0671
17011	0.0275	0.02°8	0.0268	0.0585	0 0679
19612	0 0269	0 0296	0 0253	0.0575	0.0664
20788	0.0265	0.0291	0.0251	0.0578	0.0677
22961	0.0260	0.0292	0 0251	0.0564	0.0667
24941	0.0255	0.0284	0 0244	0.0571	0.0662
26772	0.0252	0 0282	0.0246	0.0564	0.0659
28482	0.0253	0.0283	0 0243	0.0572	0 0666
30098	0 0249	0.0279	0 0241	0.0557	0.0648
31628	0 0247	0 0274	0 023°	0 055°	0 0655
33087	0 0244	0.0273	0.0238	0 0554	0.0649
34482	0.0245	0.0272	0 0234	0 0549	0.0644

TABLE 2 (CONTD)

Re	D/d = ∞ d=16 2mm	D/d=16 04 d=16 2 mm	D/d=12 05 d=16 2 mm	D/d=8 88 d=16 2 mm	D/d=6 18 d=16 2 mm
7983	0 0423	0 0474	0 0502	0 0771	0 0899
11239	0 0374	0 0466	0.0479	0 0676	0 0881
13733	0 0359	0 0461	0.0452	0 0670	0 0843
15835	0.0347	0 0389	0 0423	0 0648	0 0791
17686	0 0339	0.0387	0 0408	0 0672	0 0787
19356	0 0332	0.0359	0 0398	0 0660	0 0763
20891	0 0326	0.0363	0 0393	0 0666	0 0762
22321	0.0323	0 0366	0 0381	0 0683	0.0757
23663	0 0321	0.0346	0.0371	0 0667	0.0751
24930	0 0313	0 0351	0.0357	0 0654	0 0744
26138	0 0315	0 0356	0 0352	0 0653	0 0735
27293	0 0310	0 0346	0.0348	0.0648	0 0740
28399	0 0308	0 0334	0.0340	0.0640	0.0733

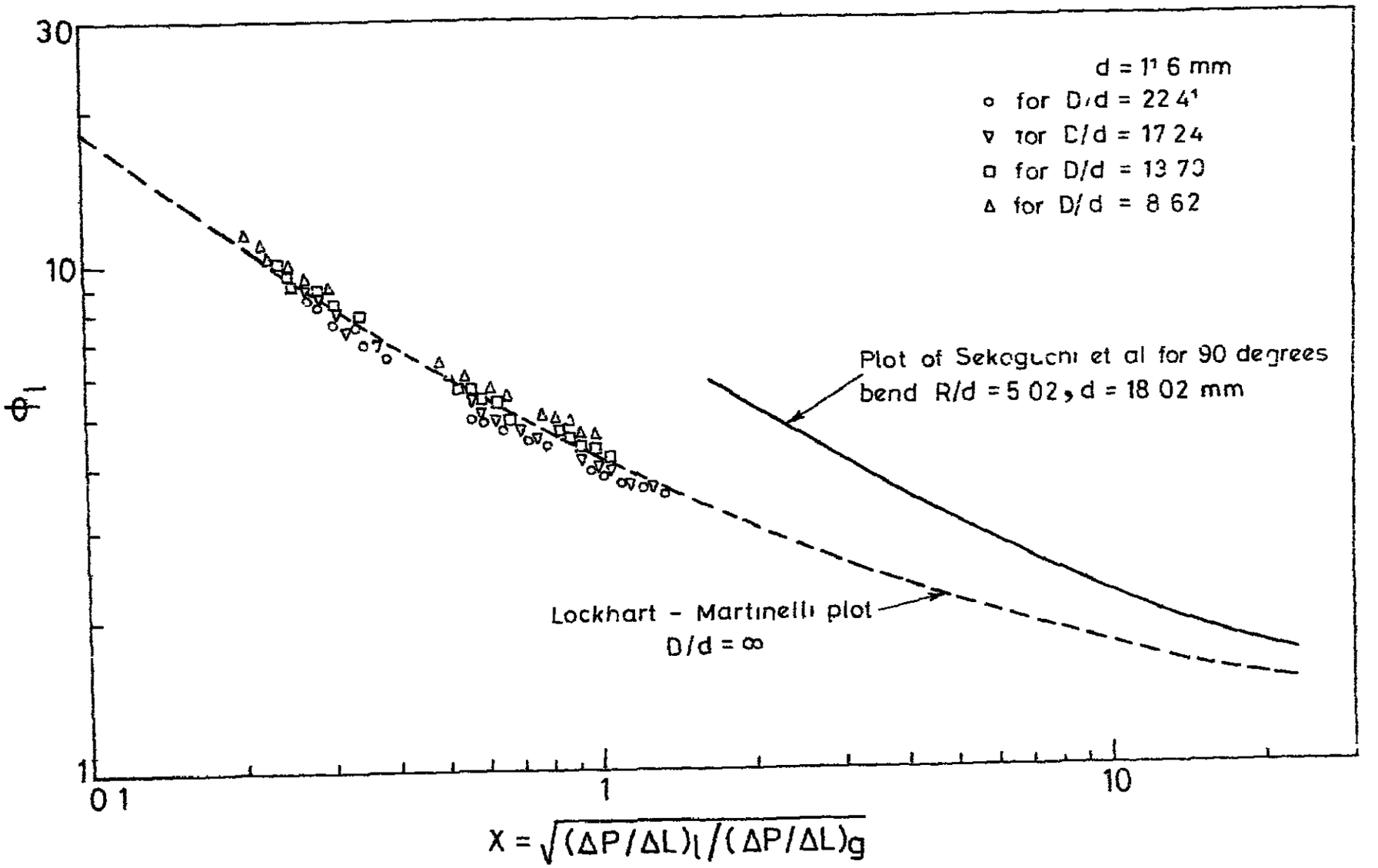
30
10
1
0 1
1
10
ϕ_l
$X = \sqrt{(\Delta P/\Delta L)_l / (\Delta P/\Delta L)_g}$
d = 1¹ 6 mm
o for D/d = 22 4¹
▽ for D/d = 17 24
□ for D/d = 13 79
△ for D/d = 8 62
Plot of Sekoguchi et al for 90 degrees bend R/d = 5 02, d = 18 02 mm
Lockhart - Martinelli plot
D/d = ∞

FIG 15 (a)

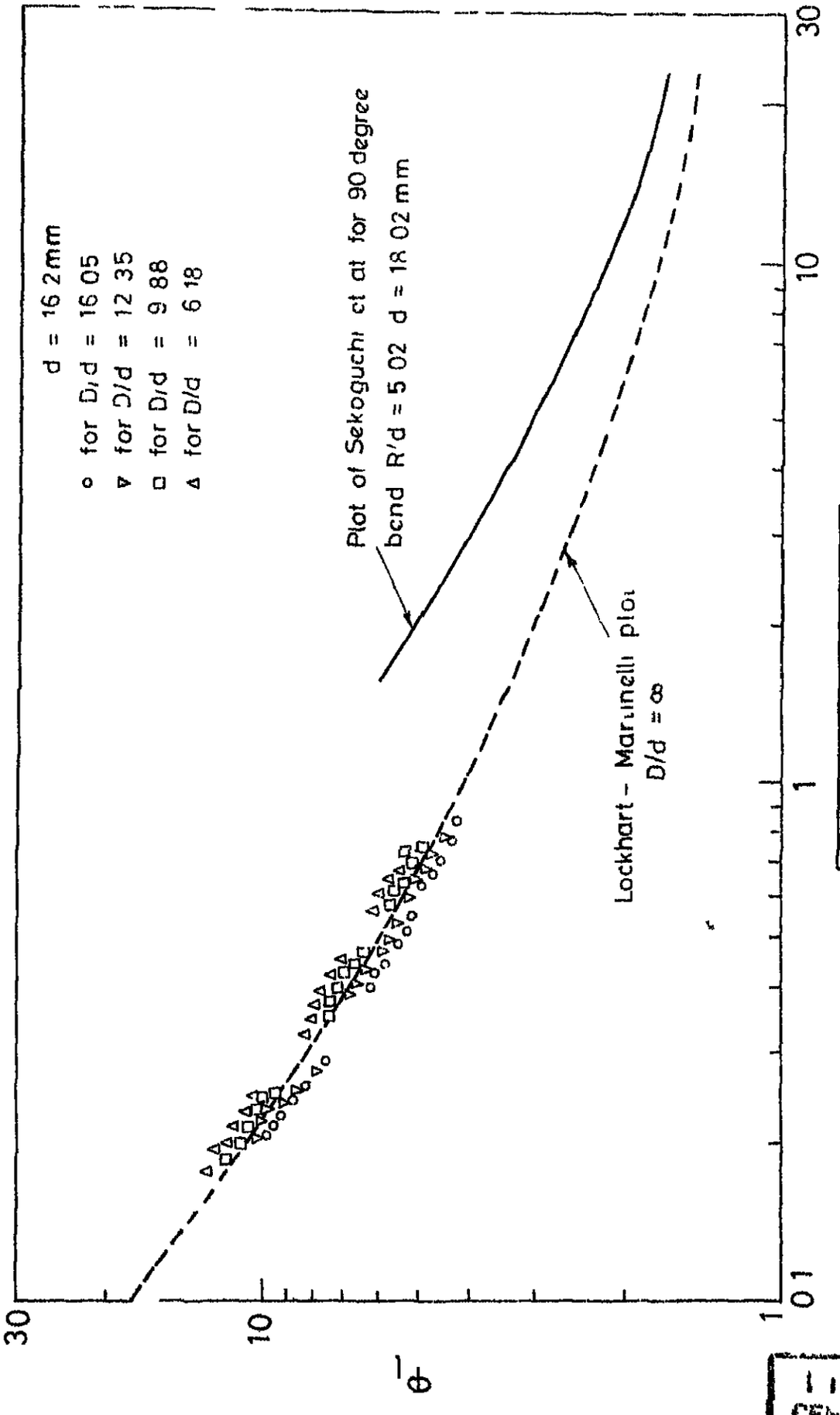

FIG 15 (b)

agrees with the observation of Hewitt et al[15] and Boyce et al[21] that the flow rate affects the Lockhart-Martinelli recommendation.

Figures 15(a) and (b) show the relationship between ϕ_1 and X for bent sections. The dotted line is the Lockhart-Martinelli plot. In these figures the plot of Sekoguchi et al[20] for 90° bends with R/d = 5.02 is also given for comparison. The present data for different D/d ratios do not separate much from each other at the flow rates involved in the experiment. Also, as the present work does not fall in the range chosen in (20) only a partial comparison between the two is possible. However it can be concluded that for the present flow conditions and geometry of the test section the Lockhart-Martinelli plot correlates the pressure drop values within ± 20% accuracy. As expected, the values of ϕ_1 decrease with increasing D/d ratios at a particular X and increase with X at a particular D/d ratio.

The present experimental results were limited to maximum air and water flow rates of 25 kg/h and 340 kg/h respectively due to the unavailability of sufficient air supply. The experiment was conducted at relatively low pressures (in the range of 1-2 atm) because of the low strength of the pressure tappings.

4.2 Error Analysis

Errors :

(a) Systematic Error - The only systematic error in the experiment may be involved in the measurement of air flow rate by orifice plate. According to Stearns et al[10] this type of measurement may carry an error of ± 8%. Moreover the readings of orifice plate were compared with that of the available rotameter for gases. It was found that the orifice plate gives a flow rate value nearly 8% lower than that of the rotameter. This suggests that the orifice plate readings might be lower than the true values. This system error affects directly the evaluation of friction factor and Reynolds number. Also the plots vs. air flow rate might be affected.

(b) Random Error -

(i) Error due to moisture in the air : The moisture content of the dry air (after passing through silica jel) was measured with the help of relative humidity sensor (Honeywell make). It was found that the relative humidity was within 15% at dry bulb temperature of 100°F. Using Psychrometric Chart the density of the sample of air was calculated. Thus knowing the density

of the moisture free air at the above conditions the error in the density of the air is about 1%. This will affect friction factor, Reynolds number and air flow rate measurement.

(ii) Error in the temperature measurement is $\pm$ 0.0515% ($= \frac{0.05}{97} \times 100$). Therefore the error involved in μ etc. due to error in temperature reading can be neglected.

(iii) Water flow measurement by Rotameter : No systematic error is made in this measurement as the rotameter was calibrated. And also the random error involved is negligible as, for the experimental purposes, the rotameter was set for some preselected flow rates like 0.1, 0.5, 1.0 and 1.5 gpm. Further, during the test there was no sensible fluctuation of the rotameter readings.

(iv) Error in the measurement of the diameter of the test section : Since commercial glass tubes were used in the test, some variation in the diameter was observed at the first decimal place in mm. However, the average measured diameters were taken as 11.6 and 16.2 mm for the two tubes. Therefore, the maximum error introduced due to a

change in diameter is $0.01/11.6 \simeq \pm 1\%$. This error affects friction factor, Reynolds number etc.

In the curved portion at some tube sections, ellipticity was observed due to the bending operation. The maximum error introduced due to noncircularity is of the order of $\pm 7\%$. This was decided by measuring the outside diameter of the curved portion. However this error cannot be added to the diameter as the appearance of ellipticity was only at some places (not throughout the bend). Again the equivalent hydraulic diameter is 0.92 times that of circular giving an error of 1.8%. But the proportional error in the pressure drop and the friction factor is within 2%. Therefore, a gross effect of 2% due to ellipticity has been accounted for.

(v) Error in the diameter of curvature of the bends : The maximum error was of the order of 3%, inclusive of that of the diameter error in bent sections. This affects the length dimension of the curved section.

(vi) The error introduced in the measurement of the length of straight section may be neglected as it is of the order of $0.2/700 \simeq \pm 0.03\%$.

(vii) Error in the manometer reading : For single-phase flow measurement, two manometers were used depending upon the range of the readings. For readings below 2" of water, the inclined tube manometer was used for which the maximum error expected is of the order of $(\frac{0.01}{0.5} \times 100)$ 2%. And for manometer readings 2" or above, the vertical tube manometer was used. The maximum error is of the order of $(\frac{0.05}{2.0} \times 100)$ 2.5%.

Because of the fluctuation of pressure in two-phase flow, the error involved in pressure measurement is much higher than that of single-phase flow. The final manometer reading was noted as the average of the fluctuation. The maximum fluctuation of $\pm$ 0.4" of water for the range of 5" and above was observed. This inherent error of the order of 8% cannot be eliminated since the fluctuation was always present. For the higher flow rates of water the fluctuation was even higher than 0.8" of water. However, the error still lies within 8%, since the pressure drop is proportionately higher.

Estimates :

The results of the present work are as follows :

(i) Air flow rate, $\dot{m}_g$

(ii) Single phase friction factor,

$$f = \left[dP/(\rho v^2/2g_c)\right] \ (d/l)$$

$$= \left[dP/(\rho \dot{m}_g^2/2g_c)\right]\left[(\pi/4)^2 d^5/l\right]$$

(iii) Reynolds number,

$$Re_g = \left[\rho vd/\mu\right] = 4\dot{m}_g/\pi\mu d$$

(iv) Pressure gradients,

$$\left(\frac{dP}{dL}\right)_{TPF}, \quad \left(\frac{dP}{dL}\right)_{GPF}, \quad \left(\frac{dP}{dL}\right)_{LPF}$$

(v) Lockhart-Martinelli parameters,

$$X = \left[(dP/dL)_{LPF}/(dP/dL)_{GPF}\right]^{1/2}$$

$$\phi_l = \left[(dP/dL)_{TPF}/(dP/dL)_{LPF}\right]^{1/2}$$

$$\phi_g = \left[(dP/dL)_{TPF}/(dP/dL)_{GPF}\right]^{1/2}$$

Thus the errors involved are :

$$\frac{\Delta \dot{m}_g}{\dot{m}_g} = \pm \ 8\%$$

$$\frac{\Delta f}{f} = \left[\pm \frac{\Delta(dP)}{dP} \pm \frac{\Delta\rho}{\rho} \pm 2\frac{\Delta \dot{m}_g}{\dot{m}_g} \pm 5\frac{\Delta d}{d} \pm \frac{\Delta l}{l}\right]$$

$$= (\pm 2.5\% \pm 1\% \pm 2 \times 8\% \pm 5 \times 1\% \pm 0)$$

$$= \pm 24.5\% \text{ for straight portion}$$

$$= \pm 24.5\% \pm 3\% + 2\% \text{ (for ellipticity)}$$

$$= \begin{matrix} \pm 29.5\% \\ -27.5\% \end{matrix} \text{ for curved portion.}$$

$$\frac{\Delta Re}{Re} = \left(\pm \frac{\Delta \dot{m}_g}{\dot{m}_g} \pm \frac{\Delta \rho}{\rho} \pm \frac{\Delta d}{d} \right)$$

$$= (\pm 8\% \pm 1\% \pm 1\%)$$

$$= \pm 10\% \text{ for straight portion}$$

$$= \left.\begin{matrix} \pm 12\% \\ -8\% \end{matrix}\right] \text{ for curved portion}$$

$$\frac{\Delta (dP/dL)}{dP/dL} = \left(\pm \frac{\Delta (dP)}{dP} \pm \frac{\Delta \rho}{\rho} \pm \frac{\Delta d}{d} \right.$$

$$= (\pm 2.5\% \pm 1\% \pm 1\%)$$

$$= \pm 4.5\% \text{ for single-phase flow in straight portion}$$

$$= \begin{matrix} +6.5\% \\ -4.5\% \end{matrix} \text{ for single-phase flow in curved portion}$$

$$= (\pm 8\% \pm 1\% \pm 1\%)$$

$$= \pm 10\% \text{ for two-phase flow in straight portion}$$

$$= \begin{matrix} +\ 12\% \\ -\ 10\% \end{matrix} \Bigg] \quad \text{for two-phase flow in curved portion}$$

$$\frac{\Delta X}{X} = \tfrac{1}{2}\left[\pm \frac{\Delta (dP/dL)}{dP/dL} \Bigg|_{GPF} \pm \frac{\Delta (dP/dL)}{dP/dL} \Bigg|_{LPF} \right]$$

$$= \tfrac{1}{2} (\pm\ 4.5\% \quad \pm\ 4.5\%)$$

$$= \pm\ 4.5\% \quad \text{in straight portion}$$

$$= \begin{matrix} +\ 6.5\% \\ -\ 4.5\% \end{matrix} \Bigg] \text{ in curved portion}$$

$$\frac{\Delta \phi_g}{\phi_g} = \frac{\Delta \phi_1}{\phi_1} = \tfrac{1}{2}\left[\pm \frac{\Delta (dP/dL)}{dP/dL} \Bigg|_{TPF} \pm \frac{\Delta (dP/dL)}{dP/dL} \Bigg|_{LPF} \right]$$

$$= \tfrac{1}{2} (\pm\ 10\% \quad \pm\ 4.5\%)$$

$$= \pm\ 7.25\% \text{ in straight portion}$$

$$= \tfrac{1}{2} \begin{bmatrix} +12\% & +\ 6.5\% \\ -10\% & -\ 4.5\% \end{bmatrix}$$

$$= \begin{matrix} +\ 9.25\% \\ -\ 7.25\% \end{matrix} \Bigg] \text{ in curved portion}$$

4.3 Conclusion

Experiments have been carried out to observe various two-phase flow patterns and to determine pressure gradients only in the case of annular flow of air-water mixture in a series of 180 degree bends made of glass tubes of 11.6 and 16.2 mm internal diameter and D/d ratios varying from 6.28 to 22.4.

The flow patterns observed for two-phase flow in 180 degree bends are similar to those seen in horizontal pipes in two-phase flow. At a given water flow rate, the air flow rate at which the transition from one flow regime to another takes place, decreases with decreasing radius of curvature, the tube diameter remaining constant. At a particular water flow rate, the transition occurs at lower air flow rate for smaller diameter tube than for larger one. Also for fixed diameter and curvature of the tube, the transition occurs at lower flow rate of air as the water flow rate increases.

The pressure drops in bends for annular flow are correlated using the Lockhart-Martinelli parameters. The correlation between $\emptyset_1$ and X is illustrated by taking the ratio of D/d as a parameter in the manner similar to that of Sekoguchi et al[20]. It is found that for the flow conditions and the geometry considered in the present work Lockhart-Martinelli plot can predict pressure drop within 20% accuracy. The effects of liquid flow rate are observed in the results when plotted in Lockhart-Martinelli plot.

4.4 Suggestions for Further Work

This experiment can be extended for measurement of void fraction and heat transfer characteristics for two-phase flow. The above measurements including pressure drop

REFERENCES

1. White, C.M., "Stream line flow through curved pipes" Proc. Royal Soc. A123, pp 645-663(1929)
2. Martinelli, R.C., and Nelson, D.B., "Prediction of Pressure Drops during Forced Circulation Boiling of Water", Trans. ASME 70, pp 695-702 (1948)
3. Lockhart, R.W., and Martinelli, R.C., "Proposed Correlation of Data for Isothermal Two-phase Two-component Flow in Pipes", Chem. Eng. Progr. 45, pp 39-48(1949)
4. Alves George, E., "Cocurrent Liquid Gas flow in a pipeline contactor", Paper presented at SanFrancisco meeting of A.I.Ch.E., Sept. 14, (1953)
5. Baker, O., "Simultaneous flow of oil and Gas", Oil Gas J. 53, pp 185-190 (July, 1954)
6. Chenoweth, J.M., and Martin, M.W., "A Pressure Drop Correlation for Turbulent Two-phase Flow of Gas Liquid Mixtures in Horizontal pipes", Petrol Refiner 34 No.10, pp 151 (1955)
7. Petric, M., "Two-phase Air-water flow phenomena", Argonne National Laboratory Report No. 5787 (March, 1958)
8. Ito, H., "Friction Factor for turbulent flow in curved pipes", J. of Basic Eng., pp 123 (June,1959)

9. Flow Measurement Pt 5, Ch IV, Supplement on Instruments and Apparatus, ASME Power Test Code (1959)

10. Flow measurements with orifice meters by Stearns, R.F.

11. Levy, S., "Steam Slip-Theoretical Prediction from Momentum Model," Trans. ASME, Ser. C, J. Heat Transfer 82, pp 113-124 (1960)

12. Owens, W.L., "Two-phase Pressure Gradient," in International Development of Heat Transfer, Part II, pp 363-368 ASME (1961)

13. Mendler, O.J., Rathbun, A.S., Vanffuff, N.E., and Weiss, A., "National-Circulation Tests with water at 800 to 2000 psia under Nonboiling, Local Boiling, and Bulk Boiling Conditions," Trans. ASME, Ser. C., J. Heat Transfer 83, pp 261-273 (1961)

14. Marchaterre, J.F., "Two-Phase Frictional Pressure Drop Prediction from Levy's Momentum Model", Trans. ASME, Ser. C, J. Heat Transfer 83, No. 4 (1961)

15. Collier, J.C., "Pressure Drop Data for the Forced convective Flow of Steam/water Mixtures in vertical Heated and unheated Annuli", AERE-R3808 Harwell, Berks, England (1962)

16. Hewith, G.F., King, I., and Lovegrove, P.C., "Hold-up and pressure drop measurements in the two-phase annular flow of air-water mixtures", Brit.Chem.Eng., 8,5,pp 311-318 (May 1963)

17. Development in Heat Transfer, Edited by Rohsenow, W.M., The M.I.T. Press, Massachusetts, U.S.A.(1964)

18. Dukler, A.E., Mayo Hicks, III., and Cleveland, R.G., "Frictional Pressure Drop in Two-phase Flow : A, A comparison of Existing correlations for Pressure Loss and Hold up", A.I.Ch.E.J., 10, pp 38-43 (January, 1964)

19. Muscettola, M., "Two-phase Flow Pressure Drop", pp 87 in Boiling Heat Transfer and Two-phase flow by L.S. Tong, John Wiley Sons, Inc., New York (1965)

20. Sekoguchi, K., Sato, Y., and Kariyasaki, A., "The Influences of Mixtures, Bends and Exit Sections on Horizontal Two-phase Flow", Cocurrent Gas liquid flow, Edited by Edward Rhodes and Donard S. Scott., Plenum Press, New York, pp 109 (1969)

21. Boyce, B.E., Collier, J.G., and Levy, J., "Hold-up and Pressure drop measurements in the two-phase flow of air-water mixtures in Helical coils", Cocurrent Gas liquid flow, Edited by Edward Rhodes and Donard S. Scott., Plenum Press, New York, pp 203 (1969)

22. Sagas, I.I., Tobilevish, N. Yu., Tkachenko, S.I., and Petrenko, Yu. D., "Structure of Two-phase flow in vertical Annuli at low Pressure", Heat Transfer Soviet Research, Vol. 2, No. 3, pp 128 (May 1970)

23. Paleyev, I.I., Lavrent'yev, M.YE., Malyas-Malitskiy, K.P., and Agafonova, F.A., "Study of the Flow of a Gas-liquid Mixture in Curved Channels", Heat Transfer Soviet Research, Vol. 3, No. 2, pp 44 (March-April, 1971).

ME-1972-M-GIR-PRE